

1 **Title:** Muscle function and homeostasis require macrophage-derived cytokine inhibition of AKT  
2 activity in *Drosophila*

3 **Short title:** Muscle Dome controls AKT and metabolism

4 Katrin Kierdorf<sup>1, †\*</sup>, Fabian Hersperger<sup>2,3</sup>, Jessica Sharrock<sup>1, ‡</sup>, Crystal M. Vincent<sup>1</sup>, Pinar Ustaoglu<sup>1</sup>,  
5 Jiawen Dou<sup>1</sup>, Attila Gyoergy<sup>4</sup>, Olaf Groß<sup>3</sup>, Daria E. Siekhaus<sup>4</sup> and Marc S. Dionne<sup>1\*\*</sup>

6 <sup>1</sup> MRC Centre for Molecular Bacteriology and Infection and Department of Life Sciences, Imperial  
7 College London, London SW7 2AZ, United Kingdom

8 <sup>2</sup> Institute of Neuropathology, Faculty of Medicine, University of Freiburg, Breisacherstraße 64, 79106  
9 Freiburg, Germany

10 <sup>3</sup> Faculty of Biology, University of Freiburg, Freiburg, Germany

11 <sup>4</sup> Institute of Science and Technology, Am Campus 1, 3400 Klosterneuburg, Austria

12 <sup>†</sup> Current address: Institute of Neuropathology, Faculty of Medicine, University of Freiburg,  
13 Breisacherstraße 64, 79106 Freiburg, Germany

14 <sup>‡</sup> Current address: Immunology Program, Memorial Sloan-Kettering Cancer Center, New York NY  
15 10065, USA

16

17 \* Corresponding author: [katrin.kierdorf@uniklinik-freiburg.de](mailto:katrin.kierdorf@uniklinik-freiburg.de)

18 \*\* Corresponding author: [m.dionne@imperial.ac.uk](mailto:m.dionne@imperial.ac.uk)

19

20 **Keywords:** cytokine signaling, insulin-AKT signaling, metabolic homeostasis, macrophage, muscle,  
21 *JAK-STAT, unpaired*

22

23 **Abstract**

24 *Unpaired* ligands are secreted signals that act via a GP130-like receptor, *domeless*, to activate JAK-  
25 STAT signaling in *Drosophila*. Like many mammalian cytokines, *unpaireds* can be activated by  
26 infection and other stresses and can promote insulin resistance in target tissues. However, the  
27 importance of this effect in non-inflammatory physiology is unknown. Here, we identify a  
28 requirement for *unpaired*-JAK signaling as a metabolic regulator in healthy adult *Drosophila* muscle.  
29 Adult muscles show basal JAK-STAT signaling activity in the absence of any immune challenge.  
30 Macrophages are the source of much of this tonic signal. Loss of the *dome* receptor on adult muscles  
31 significantly reduces lifespan and causes local and systemic metabolic pathology. These pathologies  
32 result from hyperactivation of AKT and consequent deregulation of metabolism. Thus, we identify a  
33 cytokine signal from macrophages to muscle that controls AKT activity and metabolic homeostasis.

34 **Introduction**

35 JAK/STAT activating signals are critical regulators of many biological processes in animals. Originally  
36 described mainly in immune contexts, it has increasingly become clear that JAK/STAT signaling is also  
37 central to metabolic regulation in many tissues (Dodington et al., 2018; Villarino et al., 2017). One  
38 common consequence of activation of JAK/STAT pathways in inflammatory contexts is insulin  
39 resistance in target tissues, including muscle (Kim et al., 2013; Mashili et al., 2013). However, it is  
40 difficult to describe a general metabolic interaction between JAK/STAT and insulin signaling in  
41 mammals, due to different effects at different developmental stages, differences between acute and  
42 chronic actions, and the large number of JAKs and STATs present in mammalian genomes (Dodington  
43 et al., 2018; Mavalli et al., 2010; Nieto-Vazquez et al., 2008; Vijayakumar et al., 2013).

44 The fruit fly *Drosophila melanogaster* has a single, well-conserved JAK-STAT signaling pathway. The  
45 *unpaired* (*upd*) genes *upd1-3* encode the three known ligands for this pathway; they signal by binding  
46 to a single common GP130-like receptor, encoded by *domeless* (*dome*) (Agaisse et al., 2003; Brown et  
47 al., 2001; Chen et al., 2002). Upon ligand binding, the single JAK tyrosine kinase in *Drosophila*,  
48 encoded by *hopscotch* (*hop*), is activated; Hop then activates the single known STAT, STAT92E, which  
49 functions as a homodimer (Binari and Perrimon, 1994; Chen et al., 2002; Hou et al., 1996; Yan et al.,  
50 1996). This signaling pathway plays a wide variety of functions, including segmentation of the early  
51 embryo, regulation of hematopoiesis, maintenance and differentiation of stem cells in the gut, and  
52 immune modulation (Amoyel and Bach, 2012; Myllymaki and Ramet, 2014). Importantly, several  
53 recent studies indicate roles for *upd* cytokines in metabolic regulation; for example, the *upds* are  
54 important nutrient-responsive signals in the adult fly (Beshel et al., 2017; Rajan and Perrimon, 2012;  
55 Woodcock et al., 2015; Zhao and Karpac, 2017).

56 Here, we identify a physiological requirement for Dome signaling in adult muscle. We observe that  
57 adult muscles show significant JAK/STAT signaling activity in the absence of obvious immune  
58 challenge and macrophages seem to be a source of this signal. Inactivation of *dome* on adult muscles  
59 significantly reduces lifespan and causes muscular pathology and physiological dysfunction; these  
60 result from remarkably strong AKT hyperactivation and consequent dysregulation of metabolism. We  
61 thus describe a new role for JAK/STAT signaling in adult *Drosophila* muscle with critical importance in  
62 healthy metabolic regulation.

63 **Results**

64 ***dome* is required in adult muscle**

65 To find physiological functions of JAK/STAT signaling in the adult fly, we identified tissues with basal  
66 JAK/STAT pathway activity using a STAT-responsive GFP reporter (*10xSTAT92E-GFP*) (Bach et al.,

67 2007). The strongest reporter activity we observed was in legs and thorax. We examined flies also  
68 carrying a muscle myosin heavy chain RFP reporter (*MHC-RFP*) and observed co-localization of GFP  
69 and RFP expression in the muscles of the legs, thorax and body wall (Fig S1A). We observed strong,  
70 somewhat heterogeneous reporter expression in all the muscles of the thorax and the legs, with  
71 strong expression in various leg and jump muscles and apparently weaker expression throughout the  
72 body wall muscles and indirect flight muscles (Fig 1A).

73 *dome* encodes the only known *Drosophila* STAT-activating receptor. To investigate the physiological  
74 role of this signal, we expressed *dome*<sup>Δ</sup>, a dominant-negative version of Dome lacking the  
75 intracellular signaling domain, with a temperature-inducible muscle specific driver line (*w;tubulin-*  
76 *Gal80*<sup>ts</sup>;24B-*Gal4*) (Fig S1B) (Brown et al., 2001). Controls (24B-*Gal80*<sup>ts</sup>/+) and experimental flies (24B-  
77 *Gal80*<sup>ts</sup>>*dome*<sup>Δ</sup>) were raised at 18° until eclosion to permit Dome activity during development. Flies  
78 were then shifted to 29° to inhibit Dome activity and their lifespan was monitored. Flies with Dome  
79 signaling inhibited in adult muscles were short-lived (Fig 1B, Fig S1C). This effect was also observed,  
80 more weakly, in flies kept at 25° (Fig S1D). Upd-JAK-STAT signaling is important to maintain gut  
81 integrity, and defects in gut integrity often precede death in *Drosophila*; however, our flies did not  
82 exhibit loss of gut integrity (Fig S1E) (Jiang et al., 2009; Rera et al., 2012). To determine whether  
83 Dome inhibition caused meaningful physiological dysfunction, we assayed climbing activity in 24B-  
84 *Gal80*<sup>ts</sup>/+ control flies and 24B-*Gal80*<sup>ts</sup>>*dome*<sup>Δ</sup> flies. 24B-*Gal80*<sup>ts</sup>>*dome*<sup>Δ</sup> flies showed significantly  
85 impaired climbing compared to controls (Fig 1C). Adult muscle-specific expression of *dome*<sup>Δ</sup> with a  
86 second Gal4 line (*w;tub-Gal80*<sup>ts</sup>;Mef2-*Gal4*) gave a similar reduction in lifespan and decline in  
87 climbing activity, confirming that the defect resulted from a requirement for Dome activity in muscle  
88 (Fig S1F, G).

89 Impaired muscle function is sometimes accompanied by lipid accumulation (Baik et al., 2017).  
90 Therefore, we stained thorax muscles with the neutral lipid dye LipidTox. In 14 day old flies, we  
91 detected numerous small neutral lipid inclusions in several muscles, including the large jump muscle  
92 (TTM), of 24B-*Gal80*<sup>ts</sup>>*dome*<sup>Δ</sup> flies (Fig 1D).

### 93 Muscle *dome* activity is required for normal systemic homeostasis

94 Having observed lipid inclusions in adult muscles, we analysed the systemic metabolic state of 24B-  
95 *Gal80*<sup>ts</sup>>*dome*<sup>Δ</sup> flies. We observed significant reductions in total triglyceride, glycogen and free sugar  
96 (glucose + trehalose) in these animals (Fig 1E, F). The reduction in free sugar was not detectable in  
97 any dissected solid tissue, suggesting that it was due to a reduction in hemolymph sugar (Fig 1G).

98 Reduced hemolymph sugar could result from increased tissue glucose uptake. In this case, it should  
99 be reflected in an increased metabolic stores or metabolic rate. Since metabolic stores were  
100 decreased in our flies, we tested metabolic rate by measuring respiration. CO<sub>2</sub> production and O<sub>2</sub>  
101 consumption were both significantly increased in 24B-*Gal80*<sup>ts</sup>>*dome*<sup>Δ</sup> flies, indicating an overall  
102 increase in metabolic rate (Fig 1H).

### 103 *dome* acts via *hop* to regulate AKT activity with little effect on other nutrient signaling pathways

104 The observed metabolic changes imply differences in activity of nutrient-regulated signaling  
105 pathways in 24B-*Gal80*<sup>ts</sup>>*dome*<sup>Δ</sup> flies. Several signaling pathways respond to nutrients, or their  
106 absence, to coordinate energy consumption and storage (Britton et al., 2002; Lizcano et al., 2003;  
107 Ulgherait et al., 2014). Of these, insulin signaling via AKT is the primary driver of sugar uptake by  
108 peripheral tissues.

109 We examined the activity of these signaling mechanisms in legs (a tissue source strongly enriched in  
110 muscle) from 24B-*Gal80*<sup>ts</sup>>*dome*<sup>Δ</sup> flies. We found an extremely strong increase in abundance of the

111 60-kDa form of total and activated (S505-phosphorylated) AKT (Fig 1I, J). This change was also seen in  
112 legs from *Mef2-Gal80<sup>ts</sup>>dome<sup>A</sup>* flies, confirming that *dome* functions in muscles (Fig S1H, I). We also  
113 saw this effect in flies carrying a different insertion of the *dome<sup>A</sup>* transgene, under the control of a  
114 third muscle-specific driver, *MHC-Gal4*, though the effect was weaker (Fig S1J). These *MHC-*  
115 *Gal4>dome<sup>A</sup>* (II) animals were also short-lived relative to controls (Fig S1K).

116 Elevated total AKT could result from increased transcript abundance or changes in protein  
117 production or stability. We distinguished between these possibilities by assaying *Akt1* mRNA; *Akt1*  
118 transcript levels were elevated in *24B-Gal80<sup>ts</sup>>dome<sup>A</sup>* muscle, but only by about 75%, suggesting that  
119 the large effect on AKT protein abundance must be, at least in part, post-transcriptional (Fig S1L).  
120 Similarly, AKT hyperactivation could be driven by insulin-like peptide overexpression; however, we  
121 assayed the expression of *Ilp2-7* in whole flies and observed that none of these peptides were  
122 significantly overexpressed (Fig S1M-R).

123 Unlike AKT, the amino-acid-responsive TORC1/S6K and the starvation-responsive AMPK pathway  
124 showed no significant difference in activity in *24B-Gal80<sup>ts</sup>>dome<sup>A</sup>* flies (Fig 1K, L). However, flies with  
125 AMPK knocked down in muscle did exhibit mild AKT hyperactivation (Fig S2A).

126 To identify signaling mediators acting between Dome and AKT, we first tested activity of the MAPK-  
127 ERK pathway, which can act downstream of the JAK kinase Hop (Luo et al., 2002). We found an  
128 insignificant reduction in ERK activity in *24B-Gal80<sup>ts</sup>>dome<sup>A</sup>* flies (Fig 1M). We then assayed survival  
129 and AKT activity in flies with *hop* (JAK), *Dsor1* (MEK) and *rl* (ERK) knocked down in adult muscle. *rl*  
130 and *Dsor1* knockdown gave mild or no effect on survival and pAKT (Fig S2B, C). In contrast, *hop*  
131 knockdown phenocopied the milder *dome<sup>A</sup>* transgene with regard to survival and pAKT (Fig S2D, E).

132 We further analysed the requirement for *hop* in muscle *dome* signaling by placing *24B-Gal80<sup>ts</sup>>dome<sup>A</sup>*  
133 on a genetic background carrying the viable gain-of-function allele *hop<sup>Tum-1</sup>*. Flies carrying *hop<sup>Tum-1</sup>*  
134 alone exhibited no change in lifespan, AKT phosphorylation, or muscle lipid deposition (Fig 2A-C).  
135 However, *hop<sup>Tum-1</sup>* completely rescued lifespan and pAKT levels in *24B-Gal80<sup>ts</sup>>dome<sup>A</sup>* flies (Fig 2D, E),  
136 indicating that the physiological activity of muscle Dome is mediated via Hop and that this signal is  
137 required, but not sufficient, to control muscle AKT activity.

### 138 **Increased AKT activity causes the effects of *dome* inhibition**

139 The phenotype of *24B-Gal80<sup>ts</sup>>dome<sup>A</sup>* flies is similar to that previously described in flies with loss of  
140 function in *Pten* or *foxo* (Demontis and Perrimon, 2010; Mensah et al., 2015), suggesting that AKT  
141 hyperactivation might cause the *dome* loss of function phenotype; however, to our knowledge, direct  
142 activation of muscle AKT had not previously been analysed. We generated flies with inducible  
143 expression of activated AKT (myr-AKT) in adult muscles (*w;tubulin-Gal80<sup>ts</sup>/+;24B-Gal4/UAS-myrt-AKT*  
144 [*24B-Gal80<sup>ts</sup>>myr-AKT*]) (Stocker et al., 2002). These animals phenocopied *24B-Gal80<sup>ts</sup>>dome<sup>A</sup>* flies  
145 with regard to lifespan, climbing activity, metabolite levels, metabolic rate, and muscle lipid  
146 deposition (Fig 3A-F).

147 We concluded that AKT hyperactivation could cause the pathologies seen in *24B-Gal80<sup>ts</sup>>dome<sup>A</sup>* flies.  
148 We next tested whether reducing AKT activity could rescue *24B-Gal80<sup>ts</sup>>dome<sup>A</sup>* flies. We generated  
149 flies carrying muscle-specific inducible dominant negative dome (*UAS-dome<sup>A</sup>*) with dsRNA against  
150 *Akt1* (*UAS-AKT-IR*). These flies showed significantly longer lifespan than *24B-Gal80<sup>ts</sup>>dome<sup>A</sup>* and *24B-*  
151 *Gal80<sup>ts</sup>>AKT-IR* flies, similar to all control genotypes analyzed (Fig 3G). Dome and AKT antagonism  
152 synergised to control the mRNA level of *dome* itself, further suggesting strong mutual antagonism  
153 between these pathways (Fig S3A).

154 AKT hyperactivation should reduce FOXO transcriptional activity. To test whether this loss of FOXO  
155 activity caused some of the pathologies observed in  $24B\text{-}Gal80^{\text{ts}}\text{>}dome^{\Delta}$  flies, we increased *foxo* gene  
156 dosage by combining  $24B\text{-}Gal80^{\text{ts}}\text{>}dome^{\Delta}$  with a transgene carrying a FOXO-GFP fusion protein under  
157 the control of the endogenous *foxo* regulatory regions. These animals exhibited rescue of  
158 physiological defects and lifespan compared to  $24B\text{-}Gal80^{\text{ts}}\text{>}dome^{\Delta}$  flies (Fig 3H-J). They also  
159 exhibited increased *dome* expression (Fig S3B). The effects of these manipulations on published *foxo*  
160 target genes were mixed (Fig S3B); the strongest effect we observed was that Dome blockade  
161 increased *upd2* expression, consistent with the observation that FOXO activity inhibits *upd2*  
162 expression in muscle (none of the other genes tested have been shown to be FOXO targets in  
163 muscle) (Zhao and Karpac, 2017). This may explain some of the systemic effects of Dome blockade.

164 The effect of the *foxo* transgene was stronger than expected from a 1.5-fold increase in *foxo*  
165 expression, so we further explored the relationship between FOXO protein expression and AKT  
166 phosphorylation. We found that  $24B\text{-}Gal80^{\text{ts}}\text{>}dome^{\Delta}$  markedly increased FOXO-GFP abundance, so  
167 that the increase in total FOXO was much greater than 1.5-fold (Fig S3C). This drove an apparent  
168 feedback effect, restoring AKT in leg samples of  $foxo^{\text{GFP}}\text{; }24B\text{-}Gal80^{\text{ts}}\text{>}dome^{\Delta}$  flies to near-normal levels  
169 (Fig S3D).

## 170 **Macrophages are a relevant source of *upd* signals**

171 Plasmatocytes—*Drosophila* macrophages—are a key source of *upd3* in flies on high fat diet and in  
172 mycobacterial infection (Péan et al., 2017; Woodcock et al., 2015). Plasmatocytes also express *upd1*-  
173 3 in unchallenged flies (Chakrabarti et al., 2016). We thus tested their role in activation of muscle  
174 Dome.

175 We found plasmatocytes close to STAT-GFP-positive leg muscle (Fig 4A, B). This, and the prior  
176 published data, suggested that plasmatocytes might produce relevant levels of *dome*-activating  
177 cytokines in steady state. We then overexpressed *upd3* in plasmatocytes and observed a potent  
178 increase in muscle STAT-GFP activity (Fig 4C), confirming that plasmatocyte-derived *upd* signals were  
179 able to activate muscle Dome.

180 To determine the physiological relevance of plasmatocyte-derived signals, we assayed STAT-GFP  
181 activity in flies in which plasmatocytes had been depleted by expression of the pro-apoptotic gene  
182 *reaper* (*rpr*) using a temperature-inducible plasmatocyte-specific driver line (*w;tub-Gal80^ts;crq-Gal4*).  
183 STAT-GFP fluorescence and GFP abundance were reduced in legs of plasmatocyte-depleted flies (*crq*-  
184 *Gal80^ts>rpr*) compared to controls (*crq-Gal80^ts/+*) (Fig 4D, E). Activity was not eliminated, indicating  
185 that plasmatocytes are not the only source of muscle STAT-activating signals.

186 We then examined the lifespan of flies in which we had depleted plasmatocytes in combination with  
187 various *upd* mutations and knockdowns. Plasmatocyte depletion gave animals that were short-lived  
188 (Fig 4F). (This effect was different from that we previously reported, possibly due to changes in fly  
189 culture associated with an intervening laboratory move (Woodcock et al., 2015).) The lifespan of  
190 these animals was further reduced by combining plasmatocyte depletion with null mutations in *upd2*  
191 and *upd3*; plasmatocyte-replete *upd2* *upd3* mutants exhibited near-normal lifespan (Fig 4F).  
192 Similarly, plasmatocyte depletion drove muscle lipid accumulation, and *upd2* *upd3* mutation  
193 synergised with plasmatocyte depletion to further increase muscle lipid (Fig 4G). However, depleting  
194 plasmatocytes in *upd2* *upd3* mutants failed to recapitulate the effects of muscle Dome inhibition on  
195 whole-animal triglyceride, free sugar, and glycogen levels (Fig S4A, B). This could be due to  
196 antagonistic effects of other plasmatocyte-derived signals.

197 We attempted to pinpoint a specific Upd as the relevant physiological ligand by examining STAT-GFP  
198 activity, first testing mutants in *upd2* and *upd3* because *upd1* mutation is lethal. However, these

199 mutants, including the *upd2 upd3* double-mutant, were apparently normal (Fig S4C). We then tested  
200 plasmatocyte-specific knockdown of *upd1* and *upd3*; these animals were also essentially normal (Fig  
201 S4D), and plasmatocyte *upd1* knockdown did not reduce lifespan (Fig 4H). However, plasmatocyte-  
202 specific *upd1* knockdown gave significant compensating increases in expression of *upd2* and *upd3*  
203 (Fig 4I). In keeping with this, combining plasmatocyte-specific *upd1* knockdown with mutations in  
204 *upd2* and *upd3* reduced lifespan (Fig 4J) and also reduced STAT-GFP activity in these flies (Fig S4F).

205 Our results indicate that plasmatocytes are an important physiological source of the Upd signal  
206 driving muscle Dome activity in healthy flies, and suggest that *upd1* may be the primary relevant  
207 signal in healthy animals. However, plasmatocytes are not the only relevant source of signal, and Upd  
208 mutual regulation prevents us from pinpointing a single responsible signal.

209 **Discussion**

210 Here we show that *upd-dome* signaling in muscle acts via AKT to regulate physiological homeostasis  
211 in *Drosophila*. Loss of Dome activity in adult muscles shortens lifespan and promotes local and  
212 systemic metabolic disruption. Dome specifically regulates the level and activity of AKT; AKT hyper-  
213 activation mediates the observed pathology. Plasmatocytes are a primary source of the cytokine  
214 signal. In healthy adult flies, insulin-like peptides are the primary physiological AKT agonists. The  
215 effect we observe thus appears to be an example of a cytokine-Dome-JAK signal that impairs insulin  
216 function to permit healthy physiology.

217 Our work fits into a recent body of literature demonstrating key physiological roles for JAK-STAT  
218 activating signals in *Drosophila*. Upd1 acts locally in the brain to regulate feeding and energy storage  
219 by altering the secretion of neuropeptide F (NPF) (Beshel et al., 2017). Upd2 is released by the fat  
220 body in response to dietary triglyceride and sugar to regulate secretion of insulin-like peptides (Rajan  
221 and Perrimon, 2012). More recently, muscle-derived Upd2, under control of FOXO, has been shown  
222 to regulate production of the glucagon-like signal Akh (Zhao and Karpac, 2017). Indeed, we observe  
223 that *upd2* is upregulated in flies with Dome signaling blocked in muscle, possibly explaining some of  
224 the systemic metabolic effects we observe. Plasmatocyte-derived Upd3 in flies on a high fat diet can  
225 activate the JAK/STAT pathway in various organs including muscles and can promote insulin  
226 insensitivity (Woodcock et al., 2015). Our observation that Upd signaling is required to control AKT  
227 accumulation and thus insulin pathway activity in healthy adult muscle may explain some of these  
228 prior observations and reveals a new role for macrophage-derived cytokine signaling in healthy  
229 metabolic regulation.

230 Several recent reports have examined roles of JAK/STAT signaling in *Drosophila* muscle. In larvae,  
231 muscle JAK/STAT signaling can have an effect opposite to the one we report, with pathway loss of  
232 function resulting in reduced AKT activity (Yang and Hultmark, 2017). It is unclear whether this  
233 difference represents a difference in function between developmental stages (larva vs adult) or a  
234 difference between acute and chronic consequences of pathway inactivation. Roles in specific muscle  
235 populations have also been described: for example, JAK/STAT signaling in adult visceral muscle  
236 regulates expression of Vein, an EGF-family ligand, to control intestinal stem cell proliferation  
237 (Buchon et al., 2010; Jiang et al., 2011); the role of this system in other muscles may be analogous,  
238 controlling expression of various signals to regulate systemic physiology.

239 The roles of mammalian JAK/STAT signaling in muscle physiology are more complex, but exhibit  
240 several parallels with the fly. In mice, early muscle-specific deletion of Growth Hormone Receptor  
241 (GHR) causes several symptoms including insulin resistance, while adult muscle-specific GHR deletion  
242 causes entirely different effects, including increased metabolic rate and insulin sensitivity on a high-  
243 fat diet (Mavalli et al., 2010; Vijayakumar et al., 2013; Vijayakumar et al., 2012). GHR signals via  
244 STAT5; STAT5 deletion in adult skeletal muscle promotes muscle lipid accumulation on a high-fat diet

245 (Baik et al., 2017). Other STAT pathways can also play roles. For example, the JAK-STAT activating  
246 cytokine IL-6, which signals primarily via STAT3, increases skeletal muscle insulin sensitivity when  
247 given acutely but can drive insulin resistance when provided chronically (Nieto-Vazquez et al., 2008).  
248 STAT3 itself can promote muscle insulin resistance (Kim et al., 2013; Mashili et al., 2013). The  
249 relationship between these effects and those we have shown here, and the mechanisms regulating  
250 plasmacyte Upd production during healthy physiology, remain to be determined.

251

252 **Materials and methods**

253 ***Drosophila melanogaster stocks and culture***

254 All fly stocks were maintained on food containing 10% w/v Brewer's yeast, 8% fructose, 2% polenta  
255 and 0.8% agar supplemented with propionic acid and nipagin. Crosses for experiments were  
256 performed at 18° (for crosses with temperature inducible gene expression) or 25°. Flies were shifted  
257 to 29° after eclosion where relevant.

258 Male flies were used for all experiments.

259 The following original fly stocks were used for crosses:

<b>Fly stocks</b>	<b>Description and Origin</b>
<i>w<sup>1118</sup>; tubulin-Gal80<sup>ts</sup>/SM6a;24B-Gal4/TM6c, Sb<sup>1</sup></i>	Temperature sensitive muscle specific driver line; 24B-Gal4 a gift of Nazif Alic
<i>w<sup>1118</sup>; tubulin-Gal80<sup>ts</sup>/SM6a;Mef2-Gal4/TM6c, Sb<sup>1</sup></i>	Temperature sensitive muscle specific driver line; Mef2-Gal4 a gift of Michael Taylor
<i>w<sup>1118</sup>;UAS-dome<sup>Δ</sup>/TM6c, Sb<sup>1</sup></i>	Line for expression of a dominant-negative <i>dome</i> , gift of James Castelli-Gair Hombría
<i>w<sup>1118</sup>;UAS-dome<sup>Δ</sup>/CyO</i>	Line for expression of a dominant-negative <i>dome</i> , gift of James Castelli-Gair Hombría
<i>w<sup>1118</sup>;UAS-myr-AKT/TM6c, Sb<sup>1</sup></i>	Line for over-expression of a constitutive active (myristoylated) AKT, gift of Ernst Hafen
<i>w;UAS-AMPKα-IR</i>	VDRC KK106200
<i>w;UAS-AMPKβ-IR</i>	VDRC KK104489
<i>w;UAS-rl-IR</i>	VDRC KK109108
<i>w;UAS-Dsor1-IR</i>	VDRC KK102276
<i>w<sup>1118</sup>;foxo<sup>GFP</sup></i>	Expresses GFP-tagged <i>foxo</i> fusion protein (genomic rescue construct inserted at AttP40). Bloomington <i>Drosophila</i> Stock Center (BDSC) 38644
<i>w;UAS-AKT-IR</i>	VDRC KK103703
<i>w<sup>1118</sup>;10xSTAT92E-GFP</i>	STAT-GFP reporter line (Bach et al., 2007). BDSC #26197
<i>w<sup>1118</sup>;MHC-Gal4,MHC-RFP/SM6a</i>	Muscle specific driver line and muscle specific reporter line. Derived from BDSC #38464
<i>w upd2<sup>Δ</sup> upd3<sup>Δ</sup>;;;</i>	Gift of Bruno Lemaitre
<i>w<sup>1118</sup>;crq-Gal4/TM6c, Sb<sup>1</sup></i>	Plasmacyte specific driver line, gift of Nathalie Franc
<i>w<sup>1118</sup>;tub-Gal80<sup>ts</sup>;TM2/TM6c, Sb<sup>1</sup></i>	Line for ubiquitous expression of <i>Gal80<sup>ts</sup></i> , BDSC #7108
<i>w<sup>1118</sup>;UAS-rpr/TM6c, Sb<sup>1</sup></i>	Line for over-expression of the pro-apoptotic protein rpr. Derived from BDSC #5824
<i>w<sup>1118</sup>;UAS-CD8-mCherry</i>	Line for overexpression of a CD8-mCherry

	fusion protein. Derived from BDSC #27391
<i>w<sup>1118</sup>;;srpHemo-3xmCherry/TM6c, Sb<sup>1</sup></i>	Plasmacyte reporter line
<i>w;UAS-hop-IR</i>	VDRC GD40037
<i>w;UAS-upd1-IR/SM6a</i>	VDRC GD3282
<i>w;UAS-upd3-IR</i>	VDRC GD6811
<i>w<sup>1118</sup>;;UAS-upd3/ TM6c, Sb<sup>1</sup></i>	Line for overexpression of upd3, gift of Bruce Edgar
<i>w<sup>1118</sup>;UAS-2xeGFP/ SM6a</i>	Line for expression of bicistronic GFP, BDSC #6874
<i>w<sup>1118</sup> hop<sup>Tum-L</sup>/FM7h</i>	Gain-of function mutant of <i>hop</i> ; derived by backcrossing from BDSC 8492 onto our control <i>w<sup>1118</sup></i> background

260

261 Genotype abbreviations were used for the different experimental flies in this study, in the following  
 262 table the complete genotypes are indicated:

Genotype abbreviation of flies used in the manuscript	Complete genotype of flies used in the manuscript
<i>10XSTAT92E-GFP/MHC-RFP</i>	<i>w<sup>1118</sup>;10XSTAT92E-GFP/MHC-Gal4,MHC-RFP</i>
<i>24B-Gal80<sup>ts</sup>/+</i>	<i>w<sup>1118</sup>;tub-Gal80<sup>ts</sup>/+;24B-Gal4/+</i>
<i>24B-Gal80<sup>ts</sup>&gt;dome<sup>Δ</sup></i>	<i>w<sup>1118</sup>;tub-Gal80<sup>ts</sup>/+;24B-Gal4/UAS-dome<sup>Δ</sup></i>
<i>24B-Gal80<sup>ts</sup>&gt;myr-AKT</i>	<i>w<sup>1118</sup>;tub-Gal80<sup>ts</sup>/+;24B-Gal4/UAS-myrt-AKT</i>
<i>24B-Gal80<sup>ts</sup>&gt;AMPKα-IR</i>	<i>w<sup>1118</sup>;tub-Gal80<sup>ts</sup>/UAS-AMPKα-IR;24B-Gal4/+</i>
<i>24B-Gal80<sup>ts</sup>&gt;AMPKβ-IR</i>	<i>w<sup>1118</sup>;tub-Gal80<sup>ts</sup>/UAS-AMPKβ-IR;24B-Gal4/+</i>
<i>24B-Gal80<sup>ts</sup>&gt;rl-IR</i>	<i>w<sup>1118</sup>;tub-Gal80<sup>ts</sup>/UAS-rl-IR;24B-Gal4/+</i>
<i>24B-Gal80<sup>ts</sup>&gt;Dsor1-IR</i>	<i>w<sup>1118</sup>;tub-Gal80<sup>ts</sup>/UAS-Dsor1-IR;24B-Gal4/+</i>
<i>24B-Gal80&gt;hop-IR</i>	<i>w<sup>1118</sup>;tub-Gal80<sup>ts</sup>/UAS-hop-IR;24B-Gal4/+</i>
<i>hop<sup>Tum-L</sup>;24B-Gal80&gt;dome<sup>Δ</sup></i>	<i>w<sup>1118</sup> hop<sup>Tum-L</sup>;tub-Gal80<sup>ts</sup>/+;24B-Gal4/UAS-dome<sup>Δ</sup></i>
<i>24B-Gal80<sup>ts</sup>&gt;AKT-IR</i>	<i>w<sup>1118</sup>;tub-Gal80<sup>ts</sup>/UAS-AKT-IR;24B-Gal4/+</i>
<i>24B-Gal80<sup>ts</sup>&gt;AKT-IR;dome<sup>Δ</sup></i>	<i>w<sup>1118</sup>;tub-Gal80<sup>ts</sup>/UAS-AKT-IR;24B-Gal4/UAS-dome<sup>Δ</sup></i>
<i>MHC-Gal4/+</i>	<i>w<sup>1118</sup>;MHC-Gal4,Mhc-RFP/+;</i>
<i>MHC-Gal4&gt;dome<sup>Δ</sup> (II)</i>	<i>w<sup>1118</sup>;MHC-Gal4,MHC-RFP/UAS-dome<sup>Δ</sup>;</i>
<i>foxo<sup>GFP</sup>;24B-Gal80<sup>ts</sup>/+</i>	<i>w<sup>1118</sup>;foxo<sup>GFP</sup>;tub-Gal80<sup>ts</sup>/+;24B-Gal4/+</i>
<i>foxo<sup>GFP</sup>;24B-Gal80<sup>ts</sup>&gt;dome<sup>Δ</sup></i>	<i>w<sup>1118</sup>;foxo<sup>GFP</sup>;tub-Gal80<sup>ts</sup>/+;24B-Gal4/UAS-dome<sup>Δ</sup></i>
<i>UAS-dome<sup>Δ</sup>/+</i>	<i>w<sup>1118</sup>;UAS-dome<sup>Δ</sup>/+</i>
<i>UAS-AKT-IR/+</i>	<i>w<sup>1118</sup>;UAS-AKT-IR/+;</i>
<i>UAS-AKT-IR;dome<sup>Δ</sup>/+</i>	<i>w<sup>1118</sup>;UAS-AKT-IR/+; UAS-dome<sup>Δ</sup>/+</i>
<i>Mef2-Gal80<sup>ts</sup>/+</i>	<i>w<sup>1118</sup>;tub-Gal80<sup>ts</sup>/+;Mef2-Gal4/+</i>
<i>Mef2-Gal80<sup>ts</sup>&gt;dome<sup>Δ</sup></i>	<i>w<sup>1118</sup>;tub-Gal80<sup>ts</sup>/+;Mef2-Gal4/UAS-dome<sup>Δ</sup></i>
<i>srpHemo-3xmCherry</i>	<i>w<sup>1118</sup>; srpHemo-3xmCherry/+</i>
<i>crq-Gal4/+</i>	<i>w<sup>1118</sup>;crq-Gal4/+</i>
<i>crq-Gal80<sup>ts</sup>&gt;rpr</i>	<i>w<sup>1118</sup>;tub-Gal80<sup>ts</sup>/+;crq-Gal4/UAS-rpr or w<sup>1118</sup>;tub-Gal80<sup>ts</sup>/+;crq-Gal4,UAS-CD8-mCherry,10xSTAT92E-GFP/UAS-rpr</i>
<i>crq-Gal80<sup>ts</sup>/+</i>	<i>w<sup>1118</sup>;tub-Gal80<sup>ts</sup>/+;crq-Gal4/+ or w<sup>1118</sup>;tub-Gal80<sup>ts</sup>/+;crq-Gal4,UAS-CD8-mCherry,10xSTAT92E-GFP/+</i>
<i>crq-Gal4/+</i>	<i>w<sup>1118</sup>;crq-Gal4,UAS-CD8-mCherry,10xSTAT92E-GFP/+</i>

<i>crq-Gal4&gt;upd1-IR</i>	<i>w<sup>1118</sup>;UAS-upd1-IR/+;crq-Gal4,UAS-CD8-mCherry,10xSTAT92E-GFP/+</i>
<i>crq-Gal4&gt;upd3-IR</i>	<i>w<sup>1118</sup>;UAS-upd3-IR/+;crq-Gal4,UAS-CD8-mCherry,10xSTAT92E-GFP/+</i>
<i>crq-Gal4&gt;upd3</i>	<i>w<sup>1118</sup>;;crq-Gal4,UAS-CD8-mCherry,10xSTAT92E-GFP/UAS-upd3</i>
<i>upd2<sup>Δ</sup> upd3<sup>Δ</sup>;crq-Gal80<sup>ts</sup>/+</i>	<i>w upd2<sup>Δ</sup> upd3<sup>Δ</sup>;tub-Gal80<sup>ts</sup>/+;crq-Gal4/+</i>
<i>upd2<sup>Δ</sup> upd3<sup>Δ</sup>;crq-Gal80<sup>ts</sup>&gt;rpr</i>	<i>w upd2<sup>Δ</sup> upd3<sup>Δ</sup>;tub-Gal80<sup>ts</sup>/+;crq-Gal4/UAS-rpr</i>
<i>upd2<sup>Δ</sup> upd3<sup>Δ</sup>;upd1-IR/+</i>	<i>w upd2<sup>Δ</sup> upd3<sup>Δ</sup>;UAS-upd1-IR/+</i>
<i>upd2<sup>Δ</sup> upd3<sup>Δ</sup>;crq-Gal4/+</i>	<i>w upd2<sup>Δ</sup> upd3<sup>Δ</sup>;;crq-Gal4/+</i>
<i>upd2<sup>Δ</sup> upd3<sup>Δ</sup>;crq-Gal4&gt;upd1-IR</i>	<i>w upd2<sup>Δ</sup> upd3<sup>Δ</sup>;UAS-upd1-IR/+;crq-Gal4/+</i>
<i>MHC<sup>YFP</sup>; srpHemo-3xmCherry</i>	<i>w<sup>1118</sup>; MHC<sup>YFP</sup>/+;srpHemo-3xmCherry/+</i>
<i>10xSTAT92E-GFP; srpHemo-3xmCherry</i>	<i>w<sup>1118</sup>; 10xSTAT92E-GFP/+;srpHemo-3xmCherry/+</i>

263

264 **Lifespan/Survival assays**

265 Male flies were collected after eclosion and groups of 20–40 age-matched flies per genotype were  
266 placed together in a vial with fly food (a cohort size of 20 is sufficient to detect a lifespan effect size  
267 of about 5% at p=0.05 with 90% confidence). All survival experiments were performed at 29°. Dead  
268 flies were counted daily. Vials were kept on their sides to minimize the possibility of death from flies  
269 becoming stuck to the food, and flies were moved to fresh food twice per week. Flies were  
270 transferred into new vials without CO<sub>2</sub> anaesthesia.

271 **Negative Geotaxis Assay/Climbing Assay**

272 Male flies were collected after eclosion and housed for 14 days in age-matched groups of around 20.  
273 The assay was performed in the morning, when flies were most active. Flies were transferred without  
274 CO<sub>2</sub> into a fresh empty vial without any food and closed with the open end of another empty vial.  
275 Flies were placed under a direct light source and allowed to adapt to the environment for 20 min.  
276 Negative geotaxis reflex was induced by tapping the flies to the bottom of the tube and allowing  
277 them to climb up for 8 seconds. After 8 seconds the vial was photographed. This test was repeated 3  
278 times per vial with 1 min breaks in between. The height each individual fly had climbed was  
279 measured in Image J and the average between all three runs per vial calculated.

280 **Staining of thorax samples**

281 For immunofluorescent staining of thorax muscles, we anaesthetized flies and removed the head,  
282 wings and abdomen from the thorax. Thorax samples were pre-fixed for 1 hour in 4% PFA rotating at  
283 room temperature. Thoraces were then halved sagitally with a razor blade and fixed for another 30  
284 minutes rotating at room temperature. Samples were washed with PBS + 0.1% Triton X-100, then  
285 blocked for 1 h in 3% bovine serum albumin (BSA) in PBS + 0.1% Triton X-100.

286 For Lipid-Tox staining, samples were washed with PBS and stained for 2 hours at room temperature  
287 with HCS Lipid Tox Deep Red (Thermo Fisher #H34477; 1:200). For Phalloidin labelling, the samples  
288 were washed in PBS after fixation and stained for 2 hours at room temperature with Alexa Fluor 488  
289 Phalloidin (Thermo Fisher #A12379, 1:20). Afterwards the samples were washed once with PBS and  
290 mounted in Fluoromount-G. All mounted samples were sealed with clear nail polish and stored at 4°  
291 until imaging.

292 **Confocal microscopy**

293 Imaging was performed in the Facility for Imaging by Light Microscopy (FILM) at Imperial College  
294 London and in the Institute of Neuropathology in Freiburg. A Leica SP5 and SP8 microscope (Leica)  
295 were used for imaging, using either the 10x/NA0.4 objective, or the 20x/NA0.5 objective. Images  
296 were acquired with a resolution of either 1024x1024 or 512x512, at a scan speed of 400Hz. Averages  
297 from 3-4 line scans were used, sequential scanning was employed where necessary and tile scanning  
298 was used in order to image whole flies. For imaging of whole live flies, the flies were anaesthetized  
299 with CO<sub>2</sub> and glued to a coverslip. Flies were kept on ice until imaging. For measuring mean  
300 fluorescence intensity, a z-stack of the muscle was performed and the stack was projected in an  
301 average intensity projection. Next the area of the muscle tissue analyzed was defined and the mean  
302 fluorescent intensity within this area was measured. Images were processed and analysed using  
303 Image J.

304 ***RNA isolation and Reverse Transcription***

305 For RNA extraction three whole flies or three thoraces were used per sample. After anaesthetisation,  
306 the flies were smashed in 100µl TRIzol (Invitrogen), followed by a chloroform extraction and  
307 isopropanol precipitation. The RNA pellet was cleaned with 70% ethanol and finally solubilized in  
308 water. After DNase treatment, cDNA synthesis was carried out using the First Strand cDNA Synthesis  
309 Kit (Thermo Scientific) and priming with random hexamers (Thermo Scientific). cDNA samples were  
310 further diluted and stored at -20° until analysis.

311 ***Quantitative Real-time PCR***

312 Quantitative Real-time PCR was performed with Sensimix SYBR Green no-ROX (Bioline) on a Corbett  
313 Rotor-Gene 6000 (Corbett). The cycling conditions used throughout the study were as follows: Hold  
314 95° for 10 min, then 45 cycles of 95° for 15s, 59° for 30s, 72° for 30s, followed by a melting curve. All  
315 calculated gene expression values were measured in arbitrary units (au) according to diluted cDNA  
316 standards run in each run and for each gene measured. All gene expression values are further  
317 normalized to the value of the loading control gene, Rpl1, prior to further analysis.

318 The following primer sequences have been used in this study:

<b><i>Gene name</i></b>	<b><i>Forward</i></b>	<b><i>Reverse</i></b>
<i>Akt1</i>	5'-cttgcgagttactggacaga-3'	5'-ggatgtcacctgaggcttg-3'
<i>Ilp2</i>	5'-atccgtattccaccacaag-3'	5'-gcggttccgatatcgagttta-3'
<i>Ilp3</i>	5'-caacgcaatgaccaagagaa-3'	5'-tgagcatctgaaccgaact-3'
<i>Ilp4</i>	5'-gaggctgattagactggactg-3'	5'-tggaccggctgcagtaac-3'
<i>Ilp5</i>	5'-gccttgatggacatgctga-3'	5'-agctatccaaatccgcca-3'
<i>Ilp6</i>	5'-cccttggcgatgtttcc-3'	5'-cacaaatcggttacgttctgc-3'
<i>Ilp7</i>	5'-cacaccgaggagggtctc-3'	5'-caatatacgccggacca-3'
<i>dome</i>	5'-cgactttcggtactccatc-3'	5'-accttgatgaggccaggat-3'
<i>upd1</i>	5'-gcacactgatttcgatacgg-3'	5'-ctggctggtgctgtttt -3'
<i>upd2</i>	5'-cggaacatcacgtgagcgaat-3'	5'-tcggcaggaaactgtactcg-3'
<i>upd3</i>	5'-actgggagaacaccgtcaat-3'	5'-gccccttggttctgttagat-3'
<i>Pepck1</i>	5'-ggataagggtggacgtgaag-3'	5'-acccctgcgaccagaact-3'
<i>Thor</i>	5'-caggaagggtgtcatctcgga-3'	5'-ggagtggtgagtagagggtt-3'
<i>InR</i>	5'-gcaccattataaccgaacc-3'	5'-ttaattcatccatgacgtgagc-3'
<i>Rpl1</i>	5'-tccacattgaagaaggct-3'	5'-ttcggatctcctcagactt-3'

319

320 ***Smurf Assay***

321 Smurf assays with blue-coloured fly food were performed to analyse gut integrity in different  
322 genotypes. Normal fly food, as described above, was supplemented with 0.1% Brilliant Blue FCF  
323 (Sigma Aldrich). Experimental flies were placed on the blue-coloured fly food at 9AM and kept on the  
324 food for 2 h at 29°. After 2 h the distribution of the dye within the fly was analysed for each  
325 individual. Flies without any blue dye were excluded, flies with a blue gut or crop were identified as  
326 “non-smurf” and flies which turned completely blue or showed distribution of blue dye outside the  
327 gut were classified as “smurf”.

328 ***Western Blot***

329 Dissected legs or thoraces from three flies were used per sample and smashed in 75µl 2x Laemmli  
330 loading buffer (100 mM Tris [pH 6.8], 20% glycerol, 4% SDS, 0.2 M DTT). Samples were stored at -80°  
331 until analysis. 7.5µl of this lysate were loaded per lane. Blue pre-stained protein standard (11-  
332 190kDa) (New England Biolabs) was used. Protein was transferred to nitrocellulose membrane (GE  
333 Healthcare). Membrane was blocked in 5% milk in TBST (TBS + 0.1% Tween-20). The following  
334 primary antibodies were used: anti-phospho(Ser505)-AKT (Cell Signal Technology (CST) 4054,  
335 1:1,000), anti-AKT (CST 4691, 1:1,000), anti-phospho(Thr172)-AMPK $\alpha$  (CST 2535, 1:1,000), anti-  
336 phospho(Thr389)-p70 S6 kinase (CST 9206, 1:1,000), anti-GFP (CST 2956, 1:1,000), anti-phospho-  
337 p44/42 MAPK (Erk1/2) (CST 4370, 1:1,000) and anti- $\alpha$ -tubulin (clone 12G10, Developmental Studies  
338 Hybridoma Bank, used as an unpurified supernatant at 1:3,000; used as a loading control for all  
339 blots). Primary antibodies were diluted in TBST containing 5% BSA and incubated over night at 4°.  
340 Secondary antibodies were HRP anti-rabbit IgG (CST 7074, 1:5,000) and HRP anti-mouse IgG (CST  
341 7076, 1:5,000). Proteins were detected with Supersignal West Pico Chemiluminescent Substrate  
342 (Thermo Scientific) or Supersignal West Femo Chemiluminescent Substrate (Thermo Scientific) using  
343 a LAS-3000 Imager (Fujifilm). Bands were quantified by densitometry using Image J. Quantifications  
344 reflect all experiments performed; representative blots from single experiments are shown.

345 ***Thin Layer Chromatography (TLC) for Triglycerides***

346 Groups of 10 flies were used per sample. After CO<sub>2</sub> anaesthesia the flies were placed in 100µl of ice-  
347 cold chloroform:methanol (3:1). Samples were centrifuged for 3 min at 13,000 rpm at 4°, and then  
348 flies were smashed with pestles followed by another centrifugation step. A set of standards were  
349 prepared using lard (Sainsbury's) in chloroform:methanol (3:1) for quantification. Samples and  
350 standards were loaded onto a silica gel glass plate (Millipore), and a solvent mix of hexane:ethyl  
351 ether (4:1) was prepared as mobile phase. Once the solvent front reached the top of the plate, the  
352 plate was dried and stained with an oxidising staining reagent containing ceric ammonium  
353 heptamolybdate (CAM) (Sigma Aldrich). For visualization of the oxidised bands, plates were baked at  
354 80° for 20 min. Baked plates were imaged with a scanner and triglyceride bands were quantified by  
355 densitometry according to the measured standards using Image J.

356 ***Measurement of Glucose, Trehalose and Glycogen***

357 5-7 day old male flies, kept at 29°, were used for the analysis. Flies were starved for 1 hr on 1% agar  
358 supplemented with 2% phosphate buffered saline (PBS) at 29° before being manually smashed in  
359 75µl TE + 0.1% Triton X-100 (Sigma Aldrich). 3 flies per sample were used. For measuring thorax,  
360 head and abdomen samples, flies were first anaesthetized with CO<sub>2</sub>. Afterwards, they were quickly  
361 transferred to 1xPBS and the head was cut off. The guts were carefully removed from thorax and  
362 abdomen and thorax were separated from each other. Afterwards the body parts were rinsed with  
363 1xPBS before smashing them in 75µl TE + 0.1% Triton X-100. All samples were incubated at 75° for  
364 20 min and stored at -80°. Samples were thawed prior to measurement and incubated at 65° for 5  
365 min to inactivate fly enzymes. A total of 10µl per sample was loaded for different measurements into  
366 flat-bottom 96-well tissue culture plates. Each fly sample was measured four times, first diluted in

367 water for calculation of background fly absorbance, second with glucose reagent (Sentinel  
368 Diagnostics) for the measurement of free glucose, third with glucose reagent plus trehalase (Sigma  
369 Aldrich) for trehalose measurement, and fourth with glucose reagent plus amyloglucosidase (Sigma  
370 Aldrich) for glycogen measurement. Plates were then incubated at 37° for 1 h before reading with a  
371 microplate reader (biochrom) at 492 nm. Quantities of glucose, trehalose and glycogen were  
372 calculated according to measured standards.

373 **Respirometry**

374 Respiration in flies was measured using a stop-flow gas-exchange system (Q-Box RP1LP Low Range  
375 Respirometer, Qubit Systems, Ontario, Canada, K7M 3L5). Ten flies from each genotype were put  
376 into an airtight glass tube and supplied with our standard fly food via a modified pipette tip. Each  
377 tube was provided with CO<sub>2</sub>-free air while the 'spent' air was concurrently flushed through the  
378 system and analysed for its CO<sub>2</sub> and O<sub>2</sub> content. All vials with flies were normalized to a control vial  
379 with food but no flies inside. In this way, evolved CO<sub>2</sub> per chamber and consumed O<sub>2</sub> per chamber  
380 were measured for each tube every ~ 44 min (the time required to go through each of the vials in  
381 sequence)

382 **Statistical analysis and handling of data**

383 For real-time quantitative PCR, TLCs, MFI quantification, western blot quantifications and  
384 colorimetric measurements for glucose, trehalose and glycogen levels an unpaired t-test was used to  
385 calculate statistical significance for all experiments. Respirometer data was analysed with a Mann-  
386 Whitney test. Lifespan/ Survival assays, where analysed with the Log-Rank and Wilcoxon test. Stars  
387 indicate statistical significance as followed: \* p<0.05, \*\* p<0.01 and \*\*\* p<0.001. All statistical tests  
388 were performed with Excel or GraphPad Prism software.

389 All replicates are biological. No outliers were omitted, and all replicates are included in quantitations  
390 (including in cases where a single representative experiment is shown). Flies were allocated into  
391 experimental groups according to their genotypes. Masking was not used. For survival experiments,  
392 typically, the 50% of flies that eclosed first from a given cross were used for an experiment. For  
393 smaller-scale experiments, flies were selected randomly from those of a given age and genotype.

394 **Acknowledgements**

395 We thank the Vienna Drosophila RNAi Center, the Bloomington Drosophila Stock Center, James  
396 Castelli-Gair Hombría, Ernst Hafen, Michael Taylor, Dan Hultmark, Nazif Alic, Bruce Edgar, and the  
397 FlyTrap collection at Yale University for flies. We are grateful to Rebecca Berdeaux, Günter Fritz,  
398 Marco Prinz, Katie Woodcock, Frederic Geissmann, and members of the South Kensington Fly Room  
399 for support, discussion and comments. We thank Maria Oberle for technical assistance. Work in the  
400 Dionne lab was supported by funding from BBSRC (BB/P000592/1, BB/L020122/2), MRC  
401 (MR/L018802/2), and the Wellcome Trust (207467/Z/17/Z). KK was supported by a DFG fellowship. JS  
402 was supported by BBSRC/GSK CASE studentship BB/L502169/1. FH was supported by the Neuromac  
403 Graduate School of the SFB/TRR167 and the DFG under Germany's Excellence Strategy (CIBSS-EXC-  
404 2189-Project ID 390939984). OG was supported by ERC Starting Grant 337689. The Facility for  
405 Imaging by Light Microscopy (FILM) at Imperial College London is part-supported by funding from the  
406 Wellcome Trust (104931/Z/14/Z) and BBSRC (BB/L015129/1).

407 **Author Contributions**

408 MSD and KK designed the project and wrote the manuscript. KK, FH, JS, CMV, PU, AG, DES and JD  
409 constructed reagents, performed the experiments and analysed the experimental data.

410

411 **References**

412

413 Agaisse, H., Petersen, U.M., Boutros, M., Mathey-Prevot, B., and Perrimon, N. (2003). Signaling role  
414 of hemocytes in Drosophila JAK/STAT-dependent response to septic injury. *Dev Cell* 5, 441-450.

415 Amoyel, M., and Bach, E.A. (2012). Functions of the Drosophila JAK-STAT pathway: Lessons from  
416 stem cells. *JAKSTAT* 1, 176-183.

417 Bach, E.A., Ekas, L.A., Ayala-Camargo, A., Flaherty, M.S., Lee, H., Perrimon, N., and Baeg, G.H. (2007).  
418 GFP reporters detect the activation of the Drosophila JAK/STAT pathway in vivo. *Gene Expr Patterns*  
419 7, 323-331.

420 Baik, M., Lee, M.S., Kang, H.J., Park, S.J., Piao, M.Y., Nguyen, T.H., and Hennighausen, L. (2017).  
421 Muscle-specific deletion of signal transducer and activator of transcription 5 augments lipid  
422 accumulation in skeletal muscle and liver of mice in response to high-fat diet. *Eur J Nutr* 56, 569-579.

423 Beshel, J., Dubnau, J., and Zhong, Y. (2017). A Leptin Analog Locally Produced in the Brain Acts via a  
424 Conserved Neural Circuit to Modulate Obesity-Linked Behaviors in Drosophila. *Cell metabolism* 25,  
425 208-217.

426 Binari, R., and Perrimon, N. (1994). Stripe-specific regulation of pair-rule genes by hopscotch, a  
427 putative Jak family tyrosine kinase in Drosophila. *Genes Dev* 8, 300-312.

428 Britton, J.S., Lockwood, W.K., Li, L., Cohen, S.M., and Edgar, B.A. (2002). Drosophila's insulin/PI3-  
429 kinase pathway coordinates cellular metabolism with nutritional conditions. *Dev Cell* 2, 239-249.

430 Brown, S., Hu, N., and Hombria, J.C. (2001). Identification of the first invertebrate interleukin  
431 JAK/STAT receptor, the Drosophila gene domeless. *Curr Biol* 11, 1700-1705.

432 Buchon, N., Broderick, N.A., Kuraishi, T., and Lemaitre, B. (2010). Drosophila EGFR pathway  
433 coordinates stem cell proliferation and gut remodeling following infection. *BMC Biol* 8, 152.

434 Chakrabarti, S., Dudzic, J.P., Li, X., Collas, E.J., Boquete, J.P., and Lemaitre, B. (2016). Remote Control  
435 of Intestinal Stem Cell Activity by Haemocytes in Drosophila. *PLoS genetics* 12, e1006089.

436 Chen, H.W., Chen, X., Oh, S.W., Marinissen, M.J., Gutkind, J.S., and Hou, S.X. (2002). mom identifies a  
437 receptor for the Drosophila JAK/STAT signal transduction pathway and encodes a protein distantly  
438 related to the mammalian cytokine receptor family. *Genes Dev* 16, 388-398.

439 Demontis, F., and Perrimon, N. (2010). FOXO/4E-BP signaling in Drosophila muscles regulates  
440 organism-wide proteostasis during aging. *Cell* 143, 813-825.

441 Dodington, D.W., Desai, H.R., and Woo, M. (2018). JAK/STAT - Emerging Players in Metabolism.  
442 *Trends Endocrinol Metab* 29, 55-65.

443 Hou, X.S., Melnick, M.B., and Perrimon, N. (1996). Marelle acts downstream of the Drosophila  
444 HOP/JAK kinase and encodes a protein similar to the mammalian STATs. *Cell* 84, 411-419.

445 Jiang, H., Grenley, M.O., Bravo, M.J., Blumhagen, R.Z., and Edgar, B.A. (2011). EGFR/Ras/MAPK  
446 signaling mediates adult midgut epithelial homeostasis and regeneration in Drosophila. *Cell Stem Cell*  
447 8, 84-95.

448 Jiang, H., Patel, P.H., Kohlmaier, A., Grenley, M.O., McEwen, D.G., and Edgar, B.A. (2009).  
449 Cytokine/Jak/Stat signaling mediates regeneration and homeostasis in the Drosophila midgut. *Cell*  
450 137, 1343-1355.

451 Kim, T.H., Choi, S.E., Ha, E.S., Jung, J.G., Han, S.J., Kim, H.J., Kim, D.J., Kang, Y., and Lee, K.W. (2013).  
452 IL-6 induction of TLR-4 gene expression via STAT3 has an effect on insulin resistance in human  
453 skeletal muscle. *Acta Diabetol* 50, 189-200.

454 Lizcano, J.M., Alrubaie, S., Kieloch, A., Deak, M., Leevers, S.J., and Alessi, D.R. (2003). Insulin-induced  
455 Drosophila S6 kinase activation requires phosphoinositide 3-kinase and protein kinase B. *Biochem J*  
456 374, 297-306.

457 Luo, H., Rose, P.E., Roberts, T.M., and Dearolf, C.R. (2002). The Hopscotch Jak kinase requires the Raf  
458 pathway to promote blood cell activation and differentiation in Drosophila. *Mol Genet Genomics*  
459 267, 57-63.

460 Mashili, F., Chibalin, A.V., Krook, A., and Zierath, J.R. (2013). Constitutive STAT3 phosphorylation  
461 contributes to skeletal muscle insulin resistance in type 2 diabetes. *Diabetes* 62, 457-465.

462 Mavalli, M.D., DiGirolamo, D.J., Fan, Y., Riddle, R.C., Campbell, K.S., van Groen, T., Frank, S.J.,  
463 Sperling, M.A., Esser, K.A., Bamman, M.M., *et al.* (2010). Distinct growth hormone receptor signaling

464 modes regulate skeletal muscle development and insulin sensitivity in mice. *J Clin Invest* 120, 4007-  
465 4020.

466 Mensah, L.B., Davison, C., Fan, S.J., Morris, J.F., Goberdhan, D.C., and Wilson, C. (2015). Fine-Tuning  
467 of PI3K/AKT Signaling by the Tumour Suppressor PTEN Is Required for Maintenance of Flight Muscle  
468 Function and Mitochondrial Integrity in Ageing Adult *Drosophila melanogaster*. *PLoS One* 10,  
469 e0143818.

470 Myllymaki, H., and Ramet, M. (2014). JAK/STAT pathway in *Drosophila* immunity. *Scand J Immunol*  
471 79, 377-385.

472 Nieto-Vazquez, I., Fernandez-Veledo, S., de Alvaro, C., and Lorenzo, M. (2008). Dual role of  
473 interleukin-6 in regulating insulin sensitivity in murine skeletal muscle. *Diabetes* 57, 3211-3221.

474 Péan, C.B., Schiebler, M., Tan, S.W.S., Sharrock, J.A., Kierdorf, K., Brown, K.P., Maserumule, M.C.,  
475 Menezes, S., Pilátová, M., Bronda, K., *et al.* (2017). Regulation of phagocyte triglyceride by a STAT-  
476 ATG2 pathway controls mycobacterial infection. *Nature communications* 8, 14642.

477 Rajan, A., and Perrimon, N. (2012). *Drosophila* cytokine unpaired 2 regulates physiological  
478 homeostasis by remotely controlling insulin secretion. *Cell* 151, 123-137.

479 Rera, M., Clark, R.I., and Walker, D.W. (2012). Intestinal barrier dysfunction links metabolic and  
480 inflammatory markers of aging to death in *Drosophila*. *Proc Natl Acad Sci U S A* 109, 21528-21533.

481 Stocker, H., Andjelkovic, M., Oldham, S., Laffargue, M., Wyman, M.P., Hemmings, B.A., and Hafen, E.  
482 (2002). Living with lethal PIP3 levels: viability of flies lacking PTEN restored by a PH domain mutation  
483 in Akt/PKB. *Science* 295, 2088-2091.

484 Ulgherait, M., Rana, A., Rera, M., Graniel, J., and Walker, D.W. (2014). AMPK modulates tissue and  
485 organismal aging in a non-cell-autonomous manner. *Cell Rep* 8, 1767-1780.

486 Vijayakumar, A., Buffin, N.J., Gallagher, E.J., Blank, J., Wu, Y., Yakar, S., and LeRoith, D. (2013).  
487 Deletion of growth hormone receptors in postnatal skeletal muscle of male mice does not alter  
488 muscle mass and response to pathological injury. *Endocrinology* 154, 3776-3783.

489 Vijayakumar, A., Wu, Y., Sun, H., Li, X., Jedd, Z., Liu, C., Schwartz, G.J., Yakar, S., and LeRoith, D.  
490 (2012). Targeted loss of GHR signaling in mouse skeletal muscle protects against high-fat diet-  
491 induced metabolic deterioration. *Diabetes* 61, 94-103.

492 Villarino, A.V., Kanno, Y., and O'Shea, J.J. (2017). Mechanisms and consequences of Jak-STAT  
493 signaling in the immune system. *Nat Immunol* 18, 374-384.

494 Woodcock, K.J., Kierdorf, K., Pouchelon, C.A., Vivancos, V., Dionne, M.S., and Geissmann, F. (2015).  
495 Macrophage-derived upd3 cytokine causes impaired glucose homeostasis and reduced lifespan in  
496 *Drosophila* fed a lipid-rich diet. *Immunity* 42, 133-144.

497 Yan, R., Small, S., Desplan, C., Dearolf, C.R., and Darnell, J.E., Jr. (1996). Identification of a Stat gene  
498 that functions in *Drosophila* development. *Cell* 84, 421-430.

499 Yang, H., and Hultmark, D. (2017). *Drosophila* muscles regulate the immune response against wasp  
500 infection via carbohydrate metabolism. *Sci Rep* 7, 15713.

501 Zhao, X., and Karpac, J. (2017). Muscle Directs Diurnal Energy Homeostasis through a Myokine-  
502 Dependent Hormone Module in *Drosophila*. *Curr Biol* 27, 1941-1955 e1946.

503

504

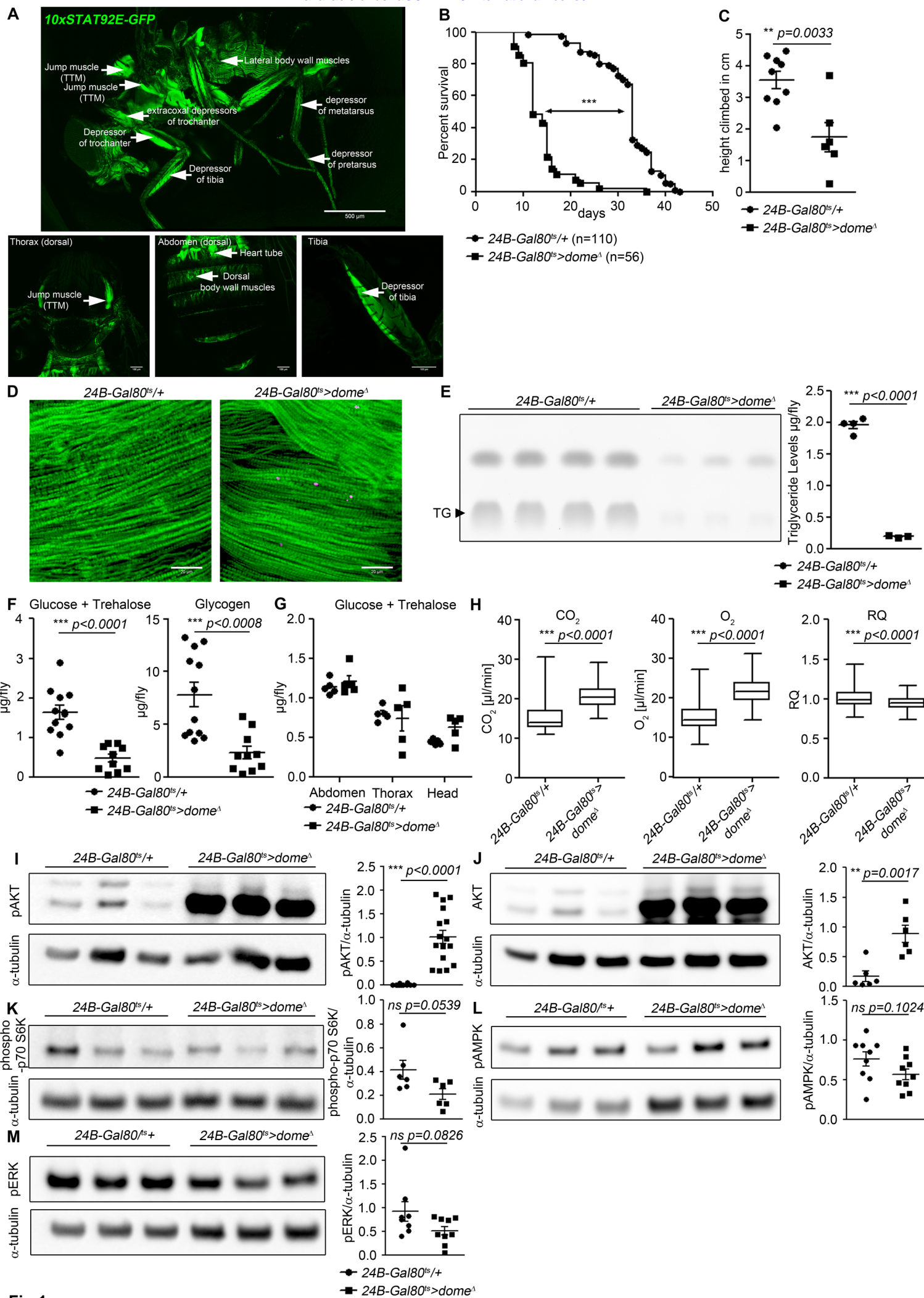


Fig 1

505 **Figure legends**

506 **Figure 1. Dome inhibition in adult muscle reduces lifespan, disrupts homeostasis, and causes AKT**  
507 **hyperactivation.**

508 A) STAT activity in different muscles in 10xSTAT92E-GFP reporter fly. One fly out of 5 shown. Upper  
509 panel: lateral view, Scale bar=500 $\mu$ m. Lower panels: dorsal thorax (left); dorsal abdomen (middle);  
510 tibia (right), Scale bar=100 $\mu$ m

511 (B) Lifespan of 24B-*Gal80*<sup>ts</sup>/+ and 24B-*Gal80*<sup>ts</sup>>*dome*<sup>Δ</sup> at 29°, pooled from three independent  
512 experiments. Log-Rank test:  $\chi^2$  =166, \*\*\* p<0.0001; Wilcoxon test:  $\chi^2$  =157.7, \*\*\* p<0.0001.

513 (C) Negative geotaxis assay of 14-day-old 24B-*Gal80*<sup>ts</sup>/+ and 24B-*Gal80*<sup>ts</sup>>*dome*<sup>Δ</sup> flies. Points  
514 represent mean height climbed in individual vials (~20 flies/vial), pooled from three independent  
515 experiments.

516 (D) Muscle (Phalloidin) and neutral lipid (LipidTox) of thorax samples from 14-day-old 24B-*Gal80*<sup>ts</sup>/+  
517 and 24B-*Gal80*<sup>ts</sup>>*dome*<sup>Δ</sup> flies. One representative fly per genotype is shown of six analysed. Scale  
518 bar=50 $\mu$ m.

519 (E) Thin layer chromatography (TLC) of triglycerides in 7-day-old 24B-*Gal80*<sup>ts</sup>/+ and 24B-  
520 *Gal80*<sup>ts</sup>>*dome*<sup>Δ</sup> flies, n=3-4 per genotype. One experiment of two is shown.

521 (F) Glucose and trehalose (left) and glycogen (right) in 7-day-old 24B-*Gal80*<sup>ts</sup>/+ and 24B-  
522 *Gal80*<sup>ts</sup>>*dome*<sup>Δ</sup> flies, pooled from two independent experiments.

523 (G) Glucose and trehalose content of dissected abdomen, thorax, and head of 7-day-old 24B-  
524 *Gal80*<sup>ts</sup>/+ and 24B-*Gal80*<sup>ts</sup>>*dome*<sup>Δ</sup> flies.

525 (H) CO<sub>2</sub> produced, O<sub>2</sub> consumed, and RQ of 7-day-old 24B-*Gal80*<sup>ts</sup>/+ and 24B-*Gal80*<sup>ts</sup>>*dome*<sup>Δ</sup> flies. Box  
526 plots show data from one representative experiment of three, with data collected from a 24 h  
527 measurement pooled from 3-4 tubes per genotype with 10 flies/tube. P values from Mann-Whitney  
528 test.

529 (I-M) Western blots of leg protein from 14-day-old 24B-*Gal80*<sup>ts</sup>/+ and 24B-*Gal80*<sup>ts</sup>>*dome*<sup>Δ</sup> flies.

530 (I) Phospho-AKT (S505). One experiment of four is shown.

531 (J) Total AKT. One experiment of two is shown.

532 (K) Phospho-p70 S6K (T398). One experiment of two is shown.

533 (L) Phospho-AMPK $\alpha$  (T173). One experiment of three is shown.

534 (M) Phospho-ERK (T202/Y204). One experiment of three is shown. P values in C, E, F, I-M from  
535 unpaired T-test.

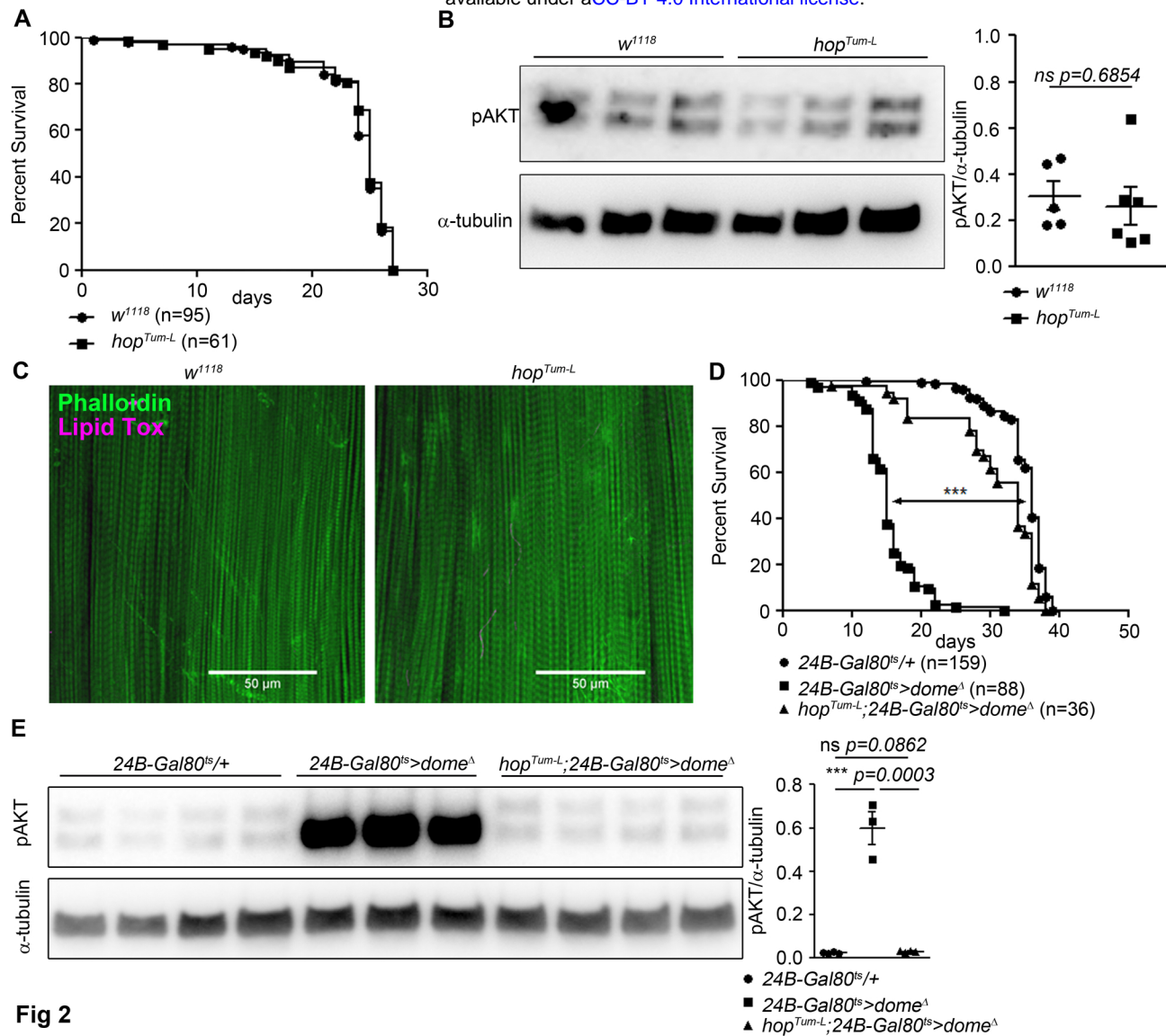


**Fig 2**

536 **Figure 2. Hop is required, but not sufficient, for Dome to control AKT.**

537 (A) Lifespan of  $w^{1118}$  and  $hop^{Tum-L}$  flies at 29°, pooled from two independent experiments. Log-Rank  
538 test:  $\chi^2 = 0.3223$ , ns p=0.5702; Wilcoxon test:  $\chi^2 = 0.4756$ , ns p=0.4906.

539 (B) Phospho-AKT in leg samples from 14-day-old  $w^{1118}$  and  $hop^{Tum-L}$  flies. One experiment of two is  
540 shown.

541 (C) Actin (Phalloidin) and neutral lipid (LipidTox) in flight muscle from 14-day-old  $w^{1118}$  and  $hop^{Tum-L}$   
542 flies. One representative fly shown of six analysed per genotype. Scale bar=50 $\mu$ m.

543 (D) Lifespan of  $24B-Gal80^{ts}/+$ ,  $24B-Gal80^{ts}>dome^A$ , and  $hop^{Tum-L};24B-Gal80^{ts}>dome^A$  flies at 29°,  
544 pooled from four independent experiments. Log-Rank test ( $24B-Gal80^{ts}/+$  vs.  $24B-Gal80^{ts}>dome^A$ ):  $\chi^2$   
545 =319.4, \*\*\* p<0.0001; Wilcoxon test ( $24B-Gal80^{ts}/+$  vs.  $24B-Gal80^{ts}>dome^A$ ):  $\chi^2$  =280.2, \*\*\* p<0.0001.  
546 Log-Rank test ( $24B-Gal80^{ts}/+$  vs.  $hop^{Tum-L} 24B-Gal80^{ts}>dome^A$ ):  $\chi^2$  =18.87, \*\*\* p<0.0001; Wilcoxon test  
547 ( $24B-Gal80^{ts}/+$  vs.  $hop^{Tum-L} 24B-Gal80^{ts}>dome^A$ ):  $\chi^2$  =20.83, \*\*\* p<0.0001.

548 (E) Phospho-AKT in leg samples from 14-day-old  $24B-Gal80^{ts}/+$ ,  $24B-Gal80^{ts}>dome^A$  and  $hop^{Tum-L};24B-$   
549  $Gal80^{ts}>dome^A$  flies. P values in B, E from unpaired T-test.

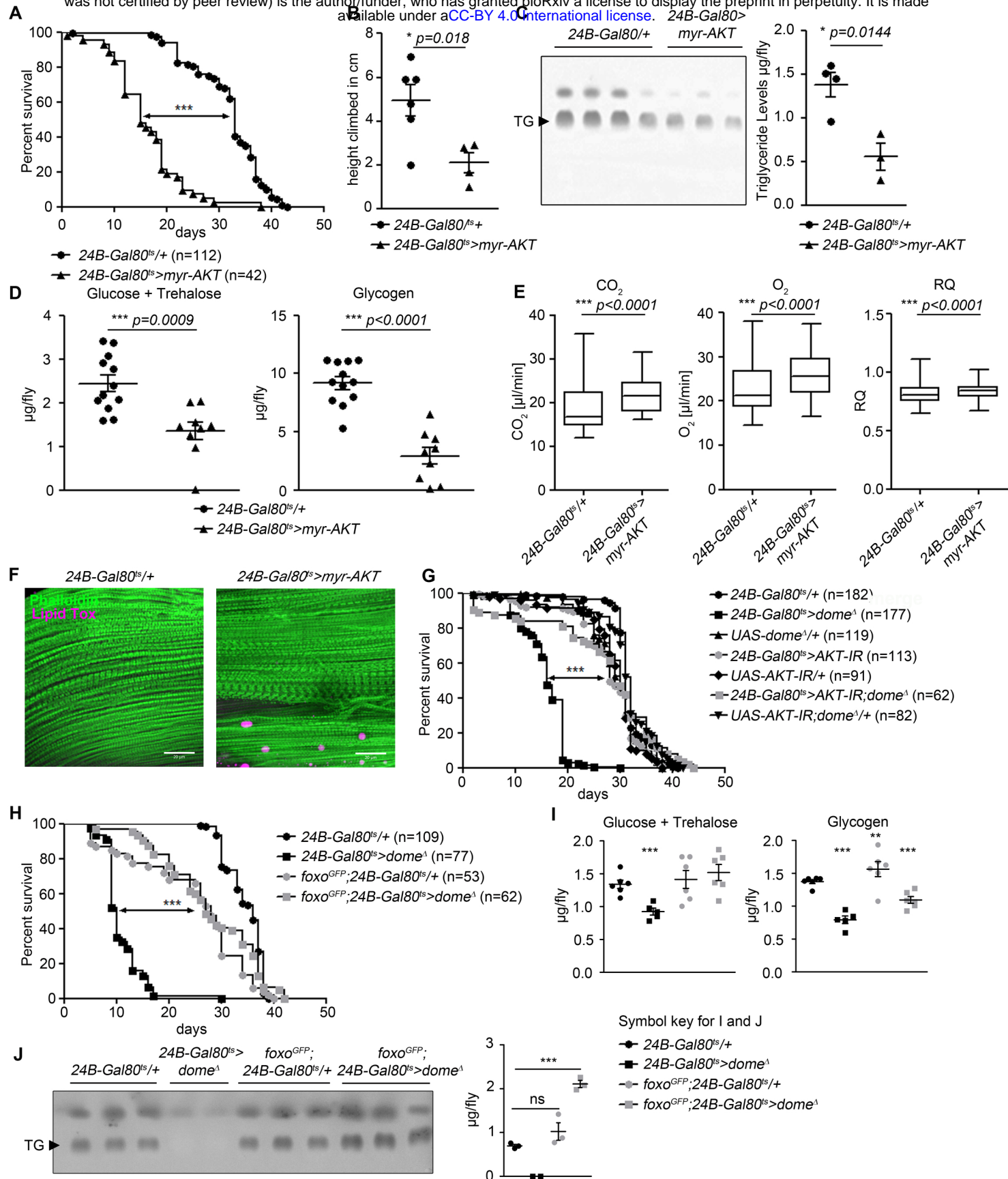


Fig 3

550 **Figure 3. AKT hyperactivation causes pathology in 24B-*Gal80<sup>ts</sup>*>*dome<sup>A</sup>* flies.**

551 (A) Lifespan of 24B-*Gal80<sup>ts</sup>*/+ and 24B-*Gal80<sup>ts</sup>*>*myr-AKT* at 29°, pooled data from three independent  
552 experiments. Log-Rank test:  $\chi^2 = 115.5$ , \*\*\* p<0.0001; Wilcoxon test:  $\chi^2 = 123.6$ , \*\*\* p<0.0001.

553 (B) Negative geotaxis assay of 14-day-old 24B-*Gal80<sup>ts</sup>*/+ and 24B-*Gal80<sup>ts</sup>*>*myr-AKT* flies. Points  
554 represent mean height climbed in individual vials (~20 flies/vial), pooled from two independent  
555 experiments.

556 (C) TLC of triglycerides in 7-day-old 24B-*Gal80<sup>ts</sup>*/+ and 24B-*Gal80<sup>ts</sup>*>*myr-AKT* flies, n=3-4 per genotype.  
557 One experiment of two is shown.

558 (D) Glucose and trehalose (left panel) and glycogen (right panel) in 7-day-old 24B-*Gal80<sup>ts</sup>*/+ (n=12)  
559 and 24B-*Gal80<sup>ts</sup>*>*myr-AKT* (n=9) flies, pooled from two independent experiments.

560 (E) CO<sub>2</sub> produced, O<sub>2</sub> consumed, and RQ of 7-day-old 24B-*Gal80<sup>ts</sup>*/+ and 24B-*Gal80<sup>ts</sup>*>*myr-AKT* flies.  
561 Box plots show data from one representative experiment of three, with data points collected from a  
562 24 h measurement pooled from 3-4 tubes per genotype with 10 flies/tube. P values from Mann-  
563 Whitney test.

564 (F) Phalloidin and LipidTox staining of thorax samples from 14-day-old 24B-*Gal80<sup>ts</sup>*/+ and 24B-  
565 *Gal80<sup>ts</sup>*>*myr-AKT* flies. One representative fly per genotype is shown of 3 analysed per group in 2  
566 independent experiments. Scale bar=50μm.

567 (G) Lifespan of 24B-*Gal80<sup>ts</sup>*/+, 24B-*Gal80<sup>ts</sup>*>*dome<sup>A</sup>*, UAS-*dome<sup>A</sup>*/+, 24B-*Gal80<sup>ts</sup>*>*AKT-IR*, UAS-*AKT-IR*/+,  
568 24B-*Gal80<sup>ts</sup>*>*AKT-IR*; *dome<sup>A</sup>* and UAS- *AKT-IR*; *dome<sup>A</sup>*/+ flies at 29°. One from four independent  
569 experiments shown. Log-Rank test (24B-*Gal80<sup>ts</sup>*>*dome<sup>A</sup>* vs. 24B-*Gal80<sup>ts</sup>*>*AKT-IR*; *dome<sup>A</sup>*):  $\chi^2 = 101.0$ ,  
570 \*\*\* p<0.0001; Wilcoxon test (24B-*Gal80<sup>ts</sup>*>*dome<sup>A</sup>* vs. 24B-*Gal80<sup>ts</sup>*>*AKT-IR*; *dome<sup>A</sup>*):  $\chi^2 = 59.87$ , \*\*\*  
571 p<0.0001.

572 (H) Lifespan of 24B-*Gal80<sup>ts</sup>*/+, 24B-*Gal80<sup>ts</sup>*>*dome<sup>A</sup>*, *foxo-GFP*; 24B-*Gal80<sup>ts</sup>*/+, and *foxo-GFP*; 24B-  
573 *Gal80<sup>ts</sup>*>*dome<sup>A</sup>* flies at 29°, pooled from three independent experiments. Log-Rank test (24B-  
574 *Gal80<sup>ts</sup>*>*dome<sup>A</sup>* vs. *foxo-GFP*; 24B-*Gal80<sup>ts</sup>*>*dome<sup>A</sup>*):  $\chi^2 = 114.0$ , \*\*\* p<0.0001; Wilcoxon test (24B-  
575 *Gal80<sup>ts</sup>*>*dome<sup>A</sup>* vs. *foxo-GFP*; 24B-*Gal80<sup>ts</sup>*>*dome<sup>A</sup>*):  $\chi^2 = 93.59$ , \*\*\* p<0.0001. 24B-*Gal80<sup>ts</sup>*/+ and 24B-  
576 *Gal80<sup>ts</sup>*>*dome<sup>A</sup>* controls in G and H are the same because a single survival experiment was split into  
577 two graphs.

578 (I) Glucose + trehalose and glycogen in 7-day-old 24B-*Gal80<sup>ts</sup>*/+, 24B-*Gal80<sup>ts</sup>*>*dome<sup>A</sup>*, *foxo-GFP*; 24B-  
579 *Gal80<sup>ts</sup>*/+, and *foxo-GFP*; 24B-*Gal80<sup>ts</sup>*>*dome<sup>A</sup>* flies.

580 (J) TLC of triglycerides in 7-day-old 24B-*Gal80<sup>ts</sup>*/+, 24B-*Gal80<sup>ts</sup>*>*dome<sup>A</sup>*, *foxo-GFP*; 24B-*Gal80<sup>ts</sup>*/+, and  
581 *foxo-GFP*; 24B-*Gal80<sup>ts</sup>*>*dome<sup>A</sup>* flies. P values in B-D, I, J from unpaired T-test.

582

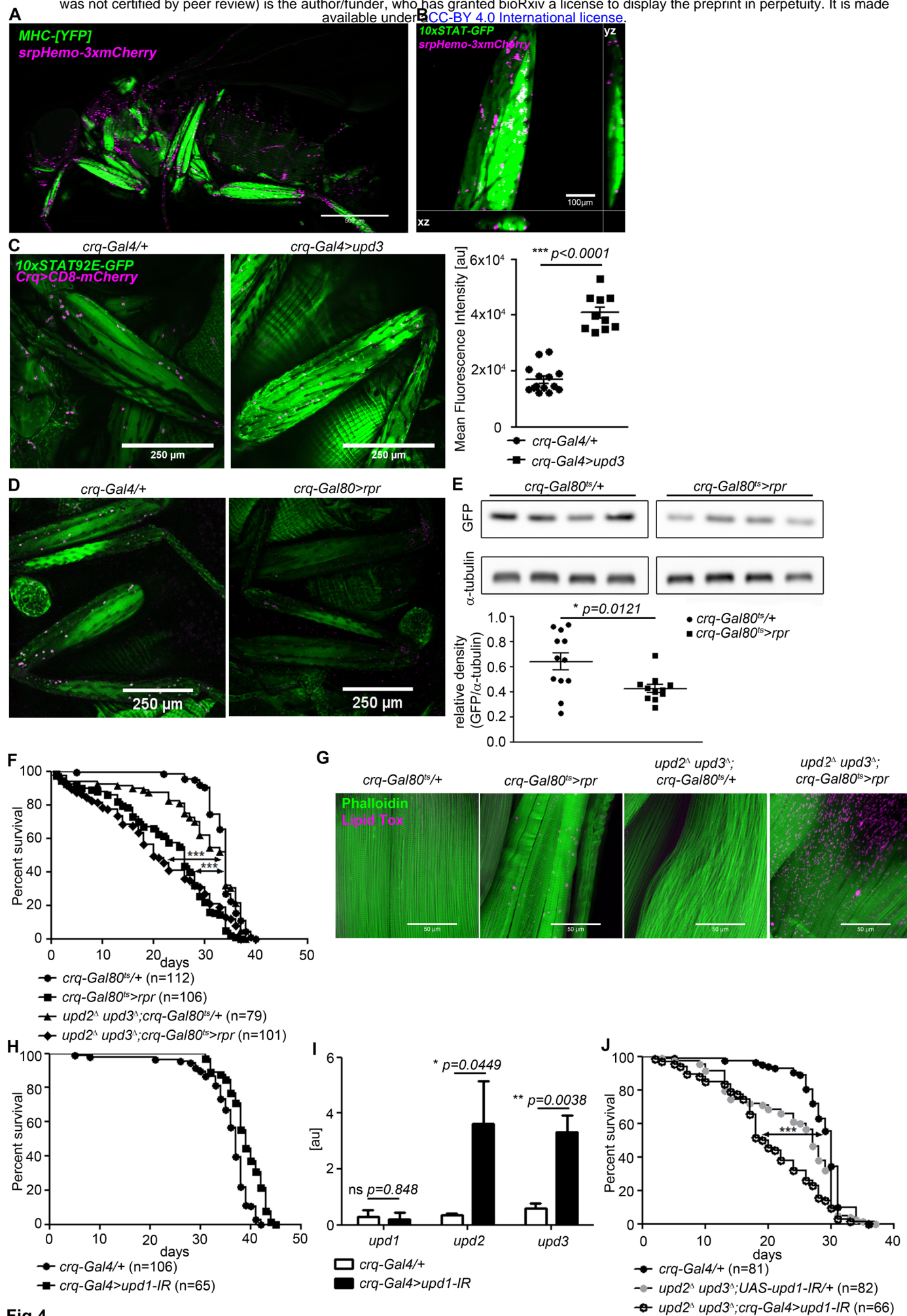


Fig 4

583 **Figure 4. Plasmatocytes promote muscle Dome activity.**

584 (A) Muscle (*MHC*<sup>YFP</sup>) and plasmatocytes (*srpHemo-3xmCherry*) in 7-day-old flies. Plasmatocytes are  
585 found in close proximity to adult muscles. One representative fly of 5 is shown. Scale bar=500 $\mu$ m.

586 (B) Legs and plasmatocytes in 7-day-old *10xSTAT92E-GFP;srpHemo-3xmCherry* flies. Muscle with high  
587 JAK-STAT activity (green) is surrounded by plasmatocytes (magenta). One representative fly of 5 is  
588 shown. Scale bar=100 $\mu$ m.

589 (C) STAT activity and plasmatocytes in legs from control (*10xSTAT92E-GFP;crq-Gal4>CD8-mCherry/+*)  
590 and *upd3*-overexpressing (*10xSTAT92E-GFP;crq-4>CD8mCherry/UAS-upd3*) flies. One representative  
591 fly of 10-14 is shown. Scale bar=100 $\mu$ m. Graph shows mean fluorescence intensity (MFI).

592 (D) STAT activity and plasmatocytes in legs from control (*10xSTAT92E-GFP;crq-Gal80<sup>ts</sup>>CD8-*  
593 *mCherry/+*) and plasmatocyte-depleted (*10xSTAT92E-GFP;crq-Gal80<sup>ts</sup>>CD8mCherry/rpr*) flies. One  
594 representative fly of six is shown. Scale bar=250 $\mu$ m.

595 (E) Western blot analysis of STAT-driven GFP in legs from 7-day-old control (*10xSTAT92E-GFP;crq-*  
596 *Gal80<sup>ts</sup>>CD8-mCherry/+*) and plasmatocyte-depleted (*10xSTAT92E-GFP;crq-Gal80<sup>ts</sup>>CD8-mCherry/rpr*  
597 flies). One representative experiment of three is shown. Graph shows STAT-GFP/α-tubulin for control  
598 (*crq-Gal80<sup>ts</sup>/+*) and plasmatocyte-depleted (*crq-Gal80<sup>ts</sup>>rpr*) leg samples.

599 (F) Lifespan of *crq-Gal80<sup>ts</sup>/+*, *crq-Gal80<sup>ts</sup>>rpr*, *upd2<sup>Δ</sup> upd3<sup>Δ</sup>;crq-Gal80<sup>ts</sup>/+*, and *upd2<sup>Δ</sup> upd3<sup>Δ</sup>;crq-*  
600 *Gal80<sup>ts</sup>>rpr* flies at 29°; pooled data from three independent experiments shown. Log-Rank test (*crq-*  
601 *Gal80<sup>ts</sup>/+* vs. *crq-Gal80<sup>ts</sup>>rpr*):  $\chi^2 = 101.7$ , \*\*\* p<0.0001; Wilcoxon test (*crq-Gal80<sup>ts</sup>/+* vs. *crq-*  
602 *Gal80<sup>ts</sup>>rpr*):  $\chi^2 = 107.8$ , \*\*\* p<0.0001; Log-Rank test (*crq-Gal80<sup>ts</sup>/+* vs. *upd2<sup>Δ</sup> upd3<sup>Δ</sup>;crq-Gal80<sup>ts</sup>>rpr*):  
603  $\chi^2 = 60.03$ , \*\*\* p<0.0001; Wilcoxon test (*crq-Gal80<sup>ts</sup>/+* vs. *upd2<sup>Δ</sup> upd3<sup>Δ</sup>;crq-Gal80<sup>ts</sup>>rpr*):  $\chi^2 = 80.97$ ,  
604 \*\*\* p<0.0001.

605 (G) Actin (Phalloidin) and neutral lipid (LipidTox) in thorax samples from 14-day-old *crq-Gal80<sup>ts</sup>/+*,  
606 *crq-Gal80<sup>ts</sup>>rpr*, *upd2<sup>Δ</sup> upd3<sup>Δ</sup>;crq-Gal80<sup>ts</sup>/+*, and *upd2<sup>Δ</sup> upd3<sup>Δ</sup>;crq-Gal80<sup>ts</sup>>rpr* flies. One  
607 representative fly per genotype shown of 6 analysed per group. Scale bar=50 $\mu$ m.

608 (H) Lifespan of *crq-Gal4/+* and *crq-Gal4>upd1-IR* flies at 29°. Log-Rank test:  $\chi^2 = 31.36$ , \*\*\* p<0.0001;  
609 Wilcoxon test:  $\chi^2 = 22.17$ , \*\*\* p=0.0001.

610 (I) Expression by qRT-PCR of *upd1*, *upd2* and *upd3* in thorax samples of *crq-Gal4/+* and *crq-*  
611 *Gal4>upd1-IR* flies, data from four independent samples of each genotype.

612 (J) Lifespan of *crq-Gal4/+*, *upd2<sup>Δ</sup> upd3<sup>Δ</sup>;UAS-upd1-IR/+*, and *upd2<sup>Δ</sup> upd3<sup>Δ</sup>;crq-Gal4>upd1-IR* flies at  
613 29°. Pooled data from three independent experiments shown. Log-Rank test (*crq-Gal4/+* vs. *upd2<sup>Δ</sup>*  
614 *upd3<sup>Δ</sup>;crq-Gal4>upd1-IR*):  $\chi^2 = 41.12$ , \*\*\* p<0.0001; Wilcoxon test (*crq-Gal4/+* vs. *upd2<sup>Δ</sup> upd3<sup>Δ</sup>;crq-*  
615 *Gal4>upd1-IR*):  $\chi^2 = 54.47$ , \*\*\* p<0.0001 Log-Rank test (*crq-Gal4/+* vs. *upd2<sup>Δ</sup> upd3<sup>Δ</sup>;UAS-upd1-IR/+*):  
616  $\chi^2 = 14.46$ , \*\*\* p<0.0001; Wilcoxon test (*crq-Gal4/+* vs. *upd2<sup>Δ</sup> upd3<sup>Δ</sup>;UAS-upd1-IR/+*):  $\chi^2 = 19.99$ , \*\*\*  
617 p<0.0001. P values in C, E, H from unpaired T-test.

618

619

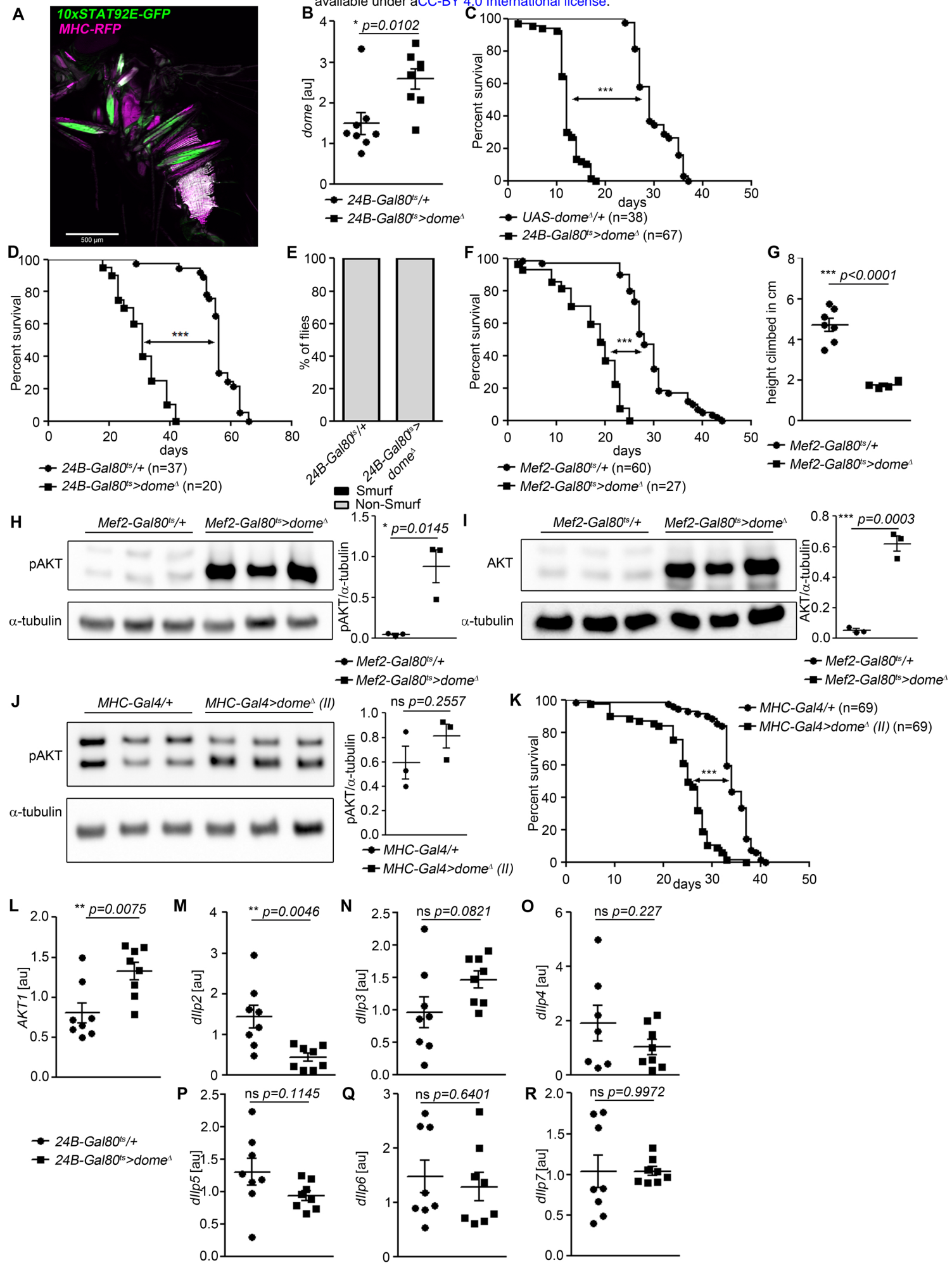


Fig S1

620 **Supplemental Information**

621 Figures S1-S4.

622

623 **Figure S1. Further characterisation of the requirement for *dome* in adult muscle.**

624 (A) STAT activity (*10xSTAT92E-GFP*) and muscle (*MHC-RFP*) colocalize in adult flies. One fly of 6  
625 shown. Scale bar=500 $\mu$ m.

626 (B) *dome* expression by qRT-PCR in thorax samples from 14-day-old *24B-Gal80<sup>ts</sup>/+* and *24B-*  
627 *Gal80<sup>ts</sup>>dome<sup>A</sup>* flies.

628 (C) Lifespan of *UAS-dome<sup>A</sup>/+* and *24B-Gal80<sup>ts</sup>>dome<sup>A</sup>* at 29°; pooled data from two independent  
629 experiments shown. Log-Rank test:  $\chi^2 = 100.8$ , \*\*\* p<0.0001; Wilcoxon test:  $\chi^2 = 76.2$ , \*\*\* p<0.0001.

630 (D) Lifespan of *24B-Gal80<sup>ts</sup>/+* and *24B-Gal80<sup>ts</sup>>dome<sup>A</sup>* at 25°; pooled data from two independent  
631 experiments shown. Log-Rank test:  $\chi^2 = 61.83$ , \*\*\* p<0.0001; Wilcoxon test:  $\chi^2 = 55.18$ , \*\*\* p<0.0001.

632 (E) Smurf assay of 14-day-old *24B-Gal80<sup>ts</sup>/+* (n=49) and *24B-Gal80<sup>ts</sup>-dome<sup>A</sup>* flies (n=18). Data pooled  
633 from two independent experiments.

634 (F) Lifespan of *Mef2-Gal80<sup>ts</sup>/+* and *Mef2-Gal80<sup>ts</sup>>dome<sup>A</sup>* flies at 29°, pooled from three independent  
635 experiments. Log-Rank test:  $\chi^2 = 86.96$ , \*\*\* p<0.0001; Wilcoxon test:  $\chi^2 = 78.61$ , \*\*\* p<0.0001.

636 (G) Negative geotaxis assay of 14-day-old *Mef2-Gal80<sup>ts</sup>/+* and *Mef2-Gal80<sup>ts</sup>>dome<sup>A</sup>* flies. Points  
637 represent mean climbing height of individual vials analysed (~20 flies/vial), pooled from three  
638 independent experiments.

639 (H, I) Western blots of protein from legs of 14-day-old *Mef2-Gal80<sup>ts</sup>/+* and *Mef2-Gal80<sup>ts</sup>>dome<sup>A</sup>* flies.  
640 One of three independent experiments is shown.

641 (H) Phospho-AKT.

642 (I) Total AKT.

643 (J) Western blots of Phospho-AKT in leg samples from 14-day-old *MHC-Gal4/+* and *MHC-Gal4>dome<sup>A</sup>*  
644 (II) flies. One of two independent experiments is shown.

645 (K) Lifespan of *MHC-Gal4/+* and *MHC-Gal4>dome<sup>A</sup>* (II) flies at 29°, pooled from two independent  
646 experiments. Log-Rank test:  $\chi^2 = 82.9$ , \*\*\* p<0.0001; Wilcoxon test:  $\chi^2 = 58.91$ , \*\*\* p<0.0001.

647 (L-R) Expression by qRT-PCR of *Akt1* and insulin-like peptides in whole fly samples from 14-day-old  
648 *24B-Gal80<sup>ts</sup>/+* and *24B-Gal80<sup>ts</sup>-dome<sup>A</sup>* flies. All transcript levels are normalized to *Rpl1* and shown in  
649 arbitrary units [au]. P values in B, G, H-J, L-R from unpaired T-test.

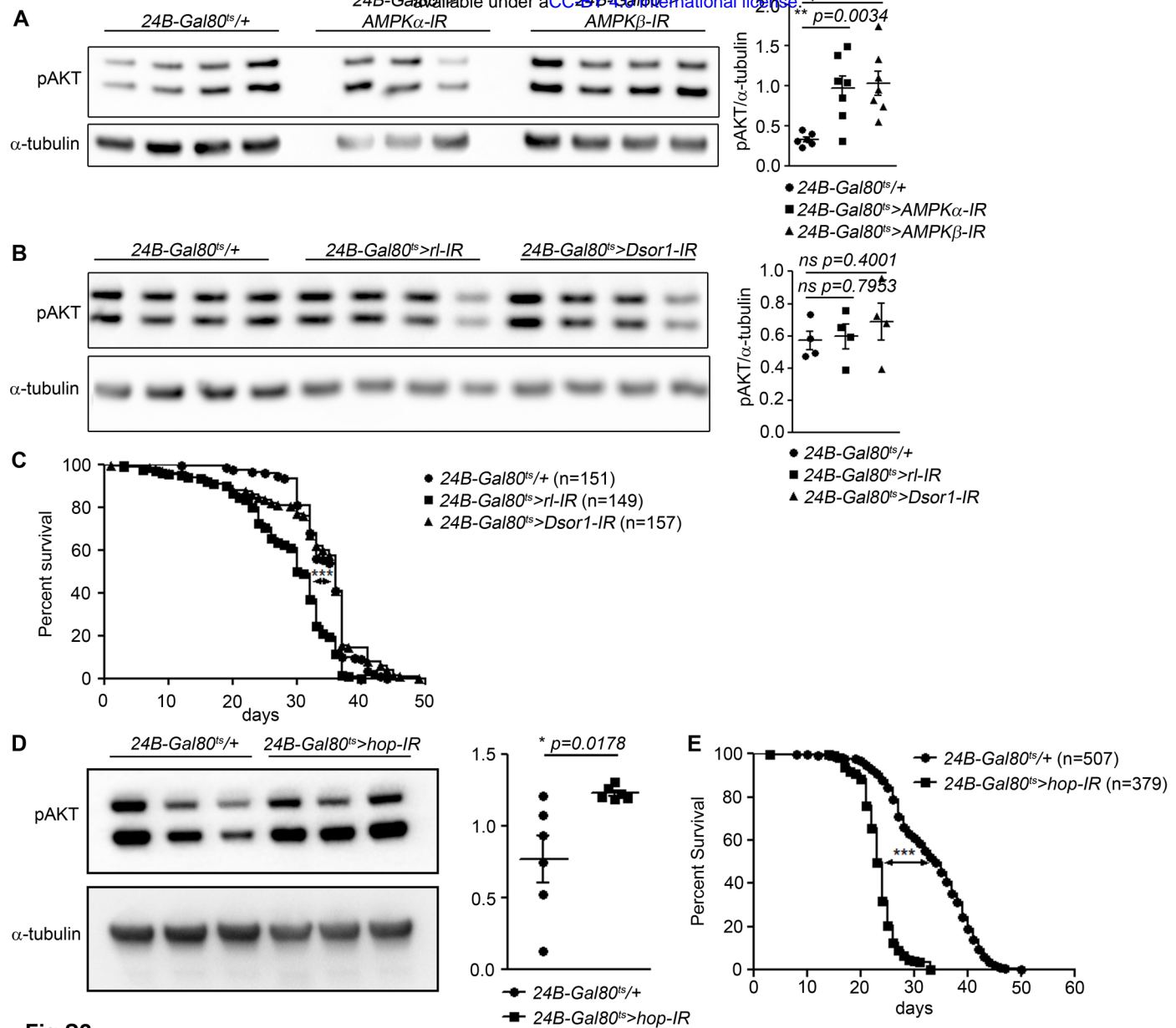


**Fig S2**

650 **Figure S2. Interactions of *dome* with AMPK, MAPK, and FOXO signaling in adult muscle.**

651 (A) Phospho-AKT in leg samples from 14-day-old *24B-Gal80<sup>ts</sup>/+*, *24B-Gal80<sup>ts</sup>>AMPK $\alpha$ -IR*, and *24B-*  
652 *Gal80<sup>ts</sup>>AMPK $\beta$ -IR* flies. One of three independent experiments is shown.

653 (B) Phospho-AKT in leg samples from 14-day-old *24B-Gal80<sup>ts</sup>/+*, *24B-Gal80<sup>ts</sup>>rl-IR*, and *24B-*  
654 *Gal80<sup>ts</sup>>Dsor1-IR* flies. One of three independent experiments is shown.

655 (C) Lifespan of *24B-Gal80<sup>ts</sup>/+*, *24B-Gal80<sup>ts</sup>>rl-IR*, and *24B-Gal80<sup>ts</sup>>Dsor1-IR* flies at 29°, pooled from  
656 four independent experiments. Log-Rank test (*24B-Gal80<sup>ts</sup>/+* vs. *24B-Gal80<sup>ts</sup>>rl-IR*):  $\chi^2 = 60.29$ , \*\*\*  
657  $p < 0.0001$ ; Wilcoxon test (*24B-Gal80<sup>ts</sup>/+* vs. *24B-Gal80<sup>ts</sup>>rl-IR*):  $\chi^2 = 58.32$ , \*\*\*  $p < 0.0001$ ; Log-Rank test  
658 (*24B-Gal80<sup>ts</sup>/+* vs. *24B-Gal80<sup>ts</sup>>Dsor1-IR*):  $\chi^2 = 1.186$ , ns  $p = 0.2760$ ; Wilcoxon test (*24B-Gal80<sup>ts</sup>/+* vs.  
659 *24B-Gal80<sup>ts</sup>>Dsor1-IR*):  $\chi^2 = 0.0033$ , ns  $p = 0.9538$ .

660 (D) Phospho-AKT in leg samples from 14-day-old *24B-Gal80<sup>ts</sup>/+* and *24B-Gal80<sup>ts</sup>>hop-IR* flies. One of  
661 two independent experiments is shown.

662 (E) Lifespan of *24B-Gal80<sup>ts</sup>/+* and *24B-Gal80<sup>ts</sup>>hop-IR* flies at 29°, pooled from four independent  
663 experiments. Log-Rank test (*24B-Gal80<sup>ts</sup>/+* vs. *24B-Gal80<sup>ts</sup>>hop-IR*):  $\chi^2 = 546.4$ , \*\*\*  $p < 0.0001$ ;  
664 Wilcoxon test (*24B-Gal80<sup>ts</sup>/+* vs. *24B-Gal80<sup>ts</sup>>hop-IR*):  $\chi^2 = 458.1$ , \*\*\*  $p < 0.0001$ . P values in A, C, E  
665 from unpaired T-test.

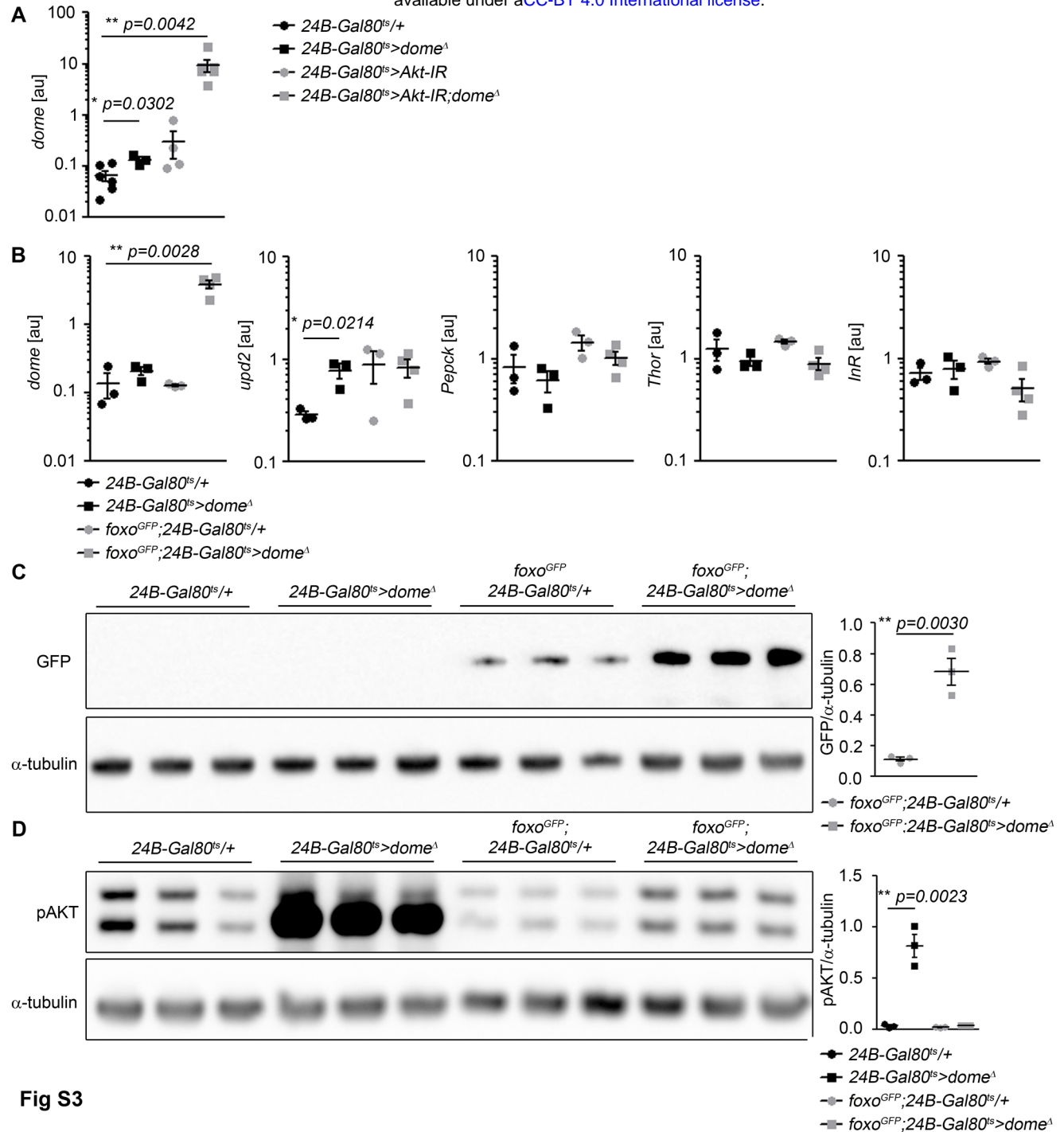


**Fig S3**

666 **Figure S3. Mutual regulation by AKT, Foxo, and Dome.**

667 (A) *dome* expression by qRT-PCR in whole fly samples from 14-day-old *24B-Gal80<sup>ts</sup>/+, 24B-*  
668 *Gal80<sup>ts</sup>>dome<sup>A</sup>*, *24B-Gal80<sup>ts</sup>>Akt-IR*, and *24B-Gal80<sup>ts</sup>>Akt-IR;dome<sup>A</sup>* flies.

669 (B) Expression by qRT-PCR of *dome*, *upd2*, *Pepck*, *Thor* and *InR* in whole fly samples from 14-day-old  
670 *24B-Gal80<sup>ts</sup>/+, 24B-Gal80<sup>ts</sup>>dome<sup>A</sup>*, *foxo-GFP;24B-Gal80<sup>ts</sup>/+*, and *foxo-GFP;24B-Gal80<sup>ts</sup>>dome<sup>A</sup>* flies.

671 (C) Western blot for GFP to detect the Foxo-GFP fusion protein in leg samples from 14-day-old *24B-*  
672 *Gal80<sup>ts</sup>/+, 24B-Gal80<sup>ts</sup>>dome<sup>A</sup>*, *foxo-GFP;24B-Gal80<sup>ts</sup>/+*, and *foxo-GFP;24B-Gal80<sup>ts</sup>>dome<sup>A</sup>* flies.

673 (D) Western blot for Phospho-AKT in leg samples from 14-day-old *24B-Gal80<sup>ts</sup>/+, 24B-Gal80<sup>ts</sup>>dome<sup>A</sup>*,  
674 *foxo-GFP;24B-Gal80<sup>ts</sup>/+*, and *foxo-GFP;24B-Gal80<sup>ts</sup>>dome<sup>A</sup>* flies. One of two independent experiments  
675 is shown. P values in A-D from unpaired T-test.

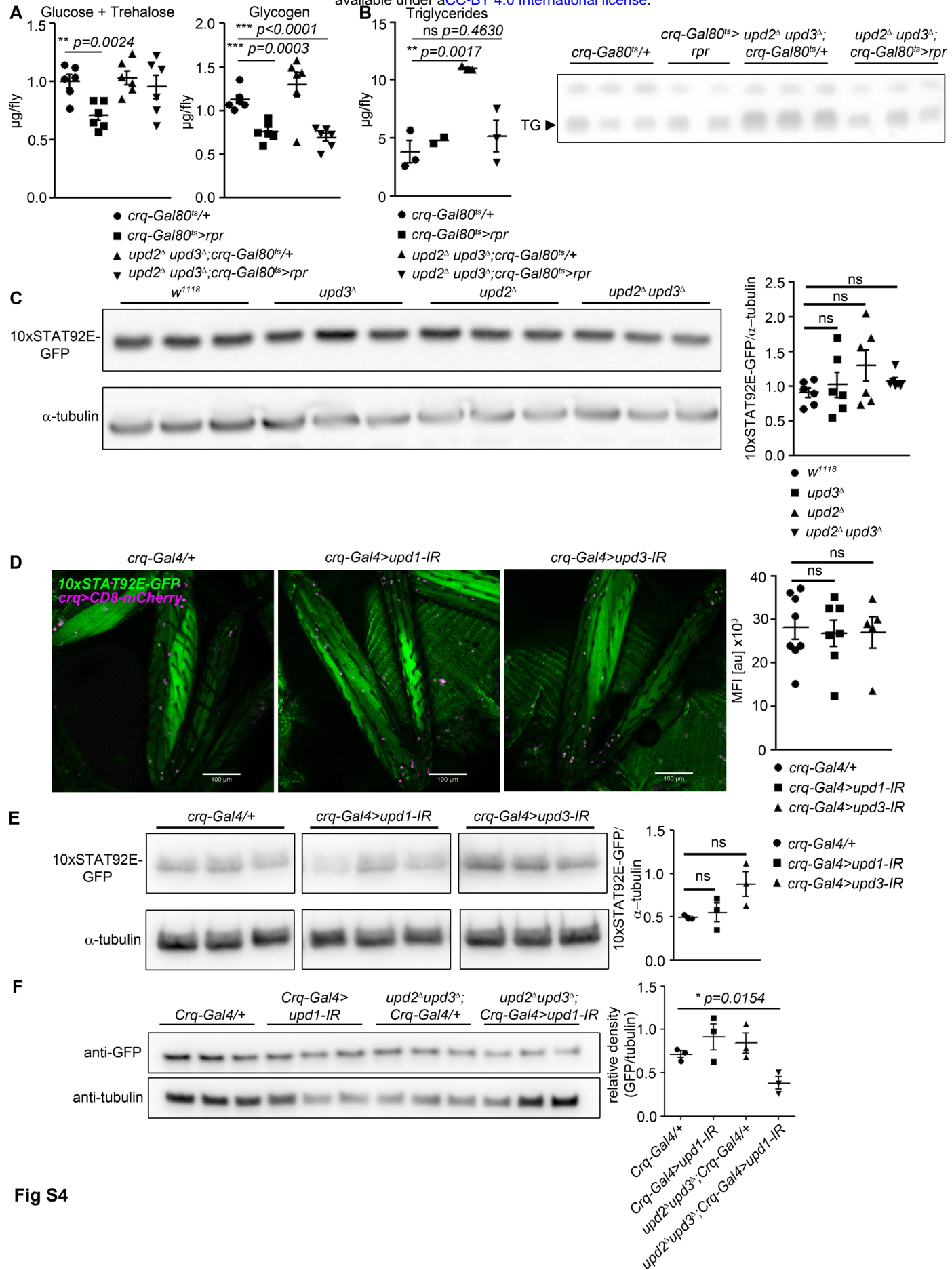


Fig S4

676 **Figure S4. Further characterisation of requirements for specific Upds.**

677 (A) Glucose + trehalose and glycogen in 7-day-old *crq-Gal80<sup>ts</sup>/+*, *crq-Gal80<sup>ts</sup>>rpr*, *upd2<sup>Δ</sup> upd3<sup>Δ</sup>;crq-*

678 *Gal80<sup>ts</sup>/+*, and *upd2<sup>Δ</sup> upd3<sup>Δ</sup>; crq-Gal80<sup>ts</sup>>rpr* flies.

679 (B) TLC of triglyceride in 7-day-old *crq-Gal80<sup>ts</sup>/+*, *crq-Gal80<sup>ts</sup>>rpr*, *upd2<sup>Δ</sup> upd3<sup>Δ</sup>;crq-Gal80<sup>ts</sup>/+*, and

680 *upd2<sup>Δ</sup> upd3<sup>Δ</sup>;crq-Gal80<sup>ts</sup>>rpr* flies, n=2-3 samples per genotype.

681 (C) Western blot analysis of STAT-driven GFP in legs from 7-day-old *w<sup>1118</sup>*, *upd3<sup>Δ</sup>*, *upd2<sup>Δ</sup>*, and *upd2<sup>Δ</sup>*

682 *upd3<sup>Δ</sup>* flies. One representative experiment of two is shown.

683 (D) STAT activity and plasmocytes in legs from 7-day-old control (*crq-Gal4/+*), *upd1* knockdown

684 (*crq-Gal4>upd1-IR*), and *upd3* knockdown (*crq-Gal4>upd3-IR*) flies. One representative fly is shown of

685 5-7 imaged for each genotype. Scale bar=100μm. Mean fluorescence intensity (MFI) is shown for all

686 flies imaged.

687 (E) Western blot analysis of STAT-driven GFP in legs from 7-day-old control (*crq-Gal4/+*), *upd1*

688 knockdown (*crq-Gal4>upd1-IR*), and *upd3* knockdown (*crq-Gal4>upd3-IR*) flies. One of two

689 independent experiments is shown.

690 (F) Western blot analysis of STAT-driven GFP in thorax from 7-day-old *crq-Gal4/+*, *crq-Gal4>upd1*,

691 *upd2<sup>Δ</sup> upd3<sup>Δ</sup>;crq-Gal4/+* and *upd2<sup>Δ</sup> upd3<sup>Δ</sup>;crq-Gal4>upd1-IR* flies. P values in A-F from unpaired T-test.

692